1.95 ± 0.07; and 11r, 1.86 ± 0.08). One-way ANOVA indicated that there was a significant effect of the number of repeats ($F_{4,35}$ = 31.6769, $P < 0.0001$). Post hoc analysis indicated that the level of luciferase activity for 6, 7, or 9r was significantly higher than that for 10 or 11r ($P < 0.01$, n = 8 in each group; Fig. 6e). In addition, two-way ANOVA indicated that there was a significant interaction between the number of repeats with Hesr2 (or the control vector; $F_{4,70}$ = 4.19, $P < 0.0045$).

Human HESR3 and mouse Hesr3 were also investigated. With human HESR3 expression, CP-Luc/exon 15 activity (6r, 1.22 ± 0.07; 7r, 1.24 ± 0.06; 9r, 1.06 ± 0.05; 10r, 1.00 ± 0.04; and 11r, 0.92 ± 0.04) was compared with the control vector (6r, 1.11 ± 0.03; 7r, 1.43 ± 0.07; 9r, 1.29 ± 0.08; 10r, 1.12 ± 0.04; and 11r, 1.06 ± 0.05). One-way ANOVA again indicated a significant effect of the number of repeats ($F_{4,35}$ = 7.0211, $P < 0.0003$). Post hoc analysis indicated that the level of luciferase activity using 6r or 7r was significantly higher than that using 10 ($P < 0.05$) or 11r ($P < 0.01$; n = 8 in each group; Fig. 6f). In addition, two-way ANOVA indicated that there was a significant interaction between the number of repeats with HESR3 or control vector ($F_{4,70}$ = 3.14, $P < 0.02$).

With the expression of mouse Hesr3, CP-Luc/exon 15 activity (6r, 1.08 ± 0.04; 7r, 1.18 ± 0.04; 9r, 1.07 ± 0.04; 10r, 1.00 ± 0.08; and 11r, 0.85 ± 0.03) was again compared with that of the control vector (6r, 1.15 ± 0.07; 7r, 1.44 ± 0.07; 9r, 1.28 ± 0.05; 10r, 1.20 ± 0.10; and 11r, 1.07 ± 0.05). One-way ANOVA indicated that there was a significant effect of the number of repeats ($F_{4,30}$ = 6.4123, $P < 0.0007$). Post hoc analysis indicated that the level of luciferase activity for 11r was significantly lower than that for 6 ($P < 0.05$), 7 ($P < 0.01$), and 9r ($P < 0.05$; n = 7 in each group; Fig. 6g). In addition, two-way ANOVA indicated no significant interaction between the number of repeats with Hesr3 or the control vector ($F_{4,65}$ = 0.67, P = 0.62). The value of luciferase expression from the each CP-Luc/exon 15 construct (6, 7, 9, 10, and 11r) with empty vector compared in Figure 6b–g was measured from same samples as used in Figure 6a.

Localization of Hesr Family Members in Mouse Midbrain

We next analyzed the localization of Hesr1, -2, and -3 by immunoperoxidase staining. Hesr1-, Hesr2-, and Hesr3-ir cells were observed in both dopaminergic and nondopaminergic regions in the mouse midbrain (Fig. 7a). Immunoreactivity against Hesr1 and -2 was observed mainly in the nucleus, whereas Hesr3 was detected in the cytoplasm (Fig. 7b). However, in the nondopaminergic regions, immunoreactivity against Hesr1 and -2 was detected in the nucleus and cytoplasm (Fig. 7c). We also analyzed the localization of Hesr family members in the TH-ir cells using double-fluorescence immunostaining. Hesr1-, Hesr2-, and Hesr3-TH-ir cells were observed in both the SN and the VTA (Fig. 8).

DISCUSSION

Roles of the 3′-UTR Including VNTR Domain for *DAT* Expression

The relative luciferase activity of CP-Luc was significantly higher than that of CP-Luc/exon 15 (10r) in SH-SY5Y cells (Fig. 3). This suggests that the 3′-UTR plays an inhibitory role in *DAT1* expression. It is possible that endogenous factors affect *DAT1* expression via the 3′-UTR; in fact, it is predicted that more than one factor binds to this region (Michelhaugh et al., 2001). Thus, we investigated the HESR family as novel candidate regulatory factors modulating *DAT1* expression.

Effects of HESR Family on the *DAT* Core Promoter

Human HESR1 and -2 or mouse Hesr1, -2, and -3 significantly decreased the relative luciferase activity level of CP-Luc containing the *DAT1* core promoter, whereas human HESR3 increased CP-Luc activity (Fig. 4). These results were unexpected, insofar as HESR1 has been identified as a 3′-UTR-binding protein. This suggests that the HESR family generally down-regulates *DAT* expression through the core promoter region. In particular, HESR1 showed strong inhibitory effects in this region, with a 36% decrease in luciferase activity with human HESR1 expression and a 39% decrease with mouse Hesr1. In fact, the core promoter region has an E-box known to be bHLH-binding consensus sites. Moreover, it has been reported that mouse *Hesr2* does not contain an E- or N-box and is repressed by Hesr proteins (Nakagawa et al., 2000). Therefore, it is likely that HESR family members recognize a binding site different from that recognized by other bHLH family members. In addition, a functional single nucleotide polymorphism (SNP; −67 A/T) in the promoter was reported to be associated with personality traits, ADHD, and bipolar disorder (Greenwood and Kelsoe, 2003; Ohadi et al., 2006, 2007; Shibuya et al., 2009). This SNP may be a point of interaction with HESR family members.

Human HESR3 was the only HESR family member that significantly increased luciferase activity of CP-Luc containing the *DAT1* core promoter. We previously reported that HESR1 containing the Leu94Met SNP in the second helix of the bHLH domain lacked inhibitory activity (Fuke et al., 2005). It was also demonstrated that this SNP dramatically transforms HESR1 from an androgen receptor corepressor to an activator (Villaronga et al., 2010). HESR3 is the only HESR with a single-amino-acid substitution adjacent to the Leu in HESR1 and -2 located in the second helix of the bHLH domain (Fig. 2). Thus, the second helix in HESR family members may be critical in the modulation of gene expression.

Effects of HESR Family on the 3′-UTR of DAT

As shown in Figure 5, human and mouse HESR1 and -2 significantly inhibited the luciferase activity of CP-Luc/exon 15 (10r). Taken together with the results shown in Figure 4, this result indicates that HESR1 and

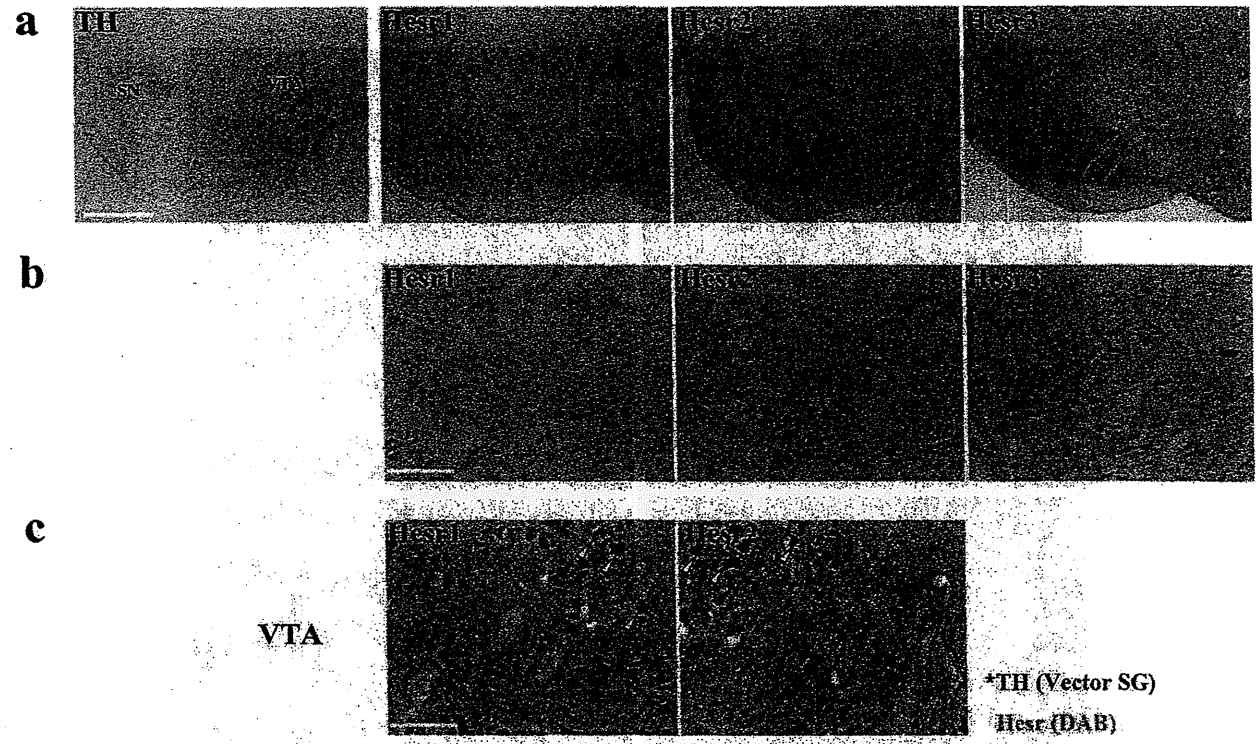

Fig. 7. Distribution of the Hesr family in mouse midbrain. Photomicrographs showing immunoperoxidase staining visualized by DAB (brown) or Vector SG (blue/gray). **a:** Localization of tyrosine hydroxylase (TH) or each Hesr family member in mouse midbrain, including the substantia nigra (SN) and ventral tegmental area (VTA). **b:** High-magnification images of the boxed areas in a. Hesr1 and -2 are localized primarily in the nucleus, whereas Hesr3 is located predominantly in the cytoplasm. **c:** Photomicrographs of the VTA and surrounding area depicting dual labeling for TH (Vector SG) and Hesr1 or 2 (DAB). Arrowheads indicate cells in which Hesr1 or -2 immunoreactivity was observed in both the nucleus and the cytoplasm. Scale bars = 500 μm in a; 100 μm in b,c.

-2 inhibit *DAT1* expression through both the core promoter and the 3′-UTR. HESR1 and -2 decreased the relative level of luciferase activity to less than 25% (HESR1) and 50% (HESR2). This degree of decrease is relatively high compared with that seen with the CP-Luc. Thus, HESR1 and -2 may have a stronger inhibitory effect on *DAT1* expression in the presence of the 3′-UTR.

We previously showed that HESR1 bound the 3′-UTR of *DAT1* directly by electromobility shift assays (Fuke et al., 2006). Because the bHLH domain is highly conserved (Steidl et al., 2000), we investigated the effect of other HESR family members to determine whether they affect gene expression by interacting with this same region. It has been proposed that more than one factor binds to this region and that the 3′-UTR, including the VNTR domain, modulates gene expression (Michelhaugh et al., 2001). Functional VNTR polymorphisms also exist in the serotonin transporter (*SERT*) gene located in intron 2, and two transcription factors, Y box-binding protein 1 (YB-1) and CCTC-binding factor (CTCF), were found to be responsible for the modulation of VNTR function (Klenova et al., 2004). This suggests that the VNTR domain functions as a modulator of gene expression (Nakamura et al., 1998) with other binding proteins.

Comparison of *DAT* Expression With the VNTR: Differential Effects of HESR Family on Each VNTR Allele

The number of repeats in the VNTR domain significantly affected the level of luciferase activity of CP-Luc/exon 15 in SH-SY5Y cells (Fig. 6a). This suggests that the VNTR domain in the *DAT* 3′-UTR is the functional sequence for *DAT* expression and is supported by in vivo neuroimaging involving SPECT (Heinz et al., 2000; Jacobsen et al., 2000; Martinez et al., 2001) and ex vivo RT-PCR analysis (Mill et al., 2002; Brookes et al., 2007). When the HESR family was transiently transfected, the number of repeats in the VNTR domain significantly affected the luciferase activity of CP-Luc/exon 15 (Fig. 6b–g). In addition, interactive effects between the number of repeats and the HESR or control vector were detected for all groups except mouse Hesr3. This suggests that the HESR

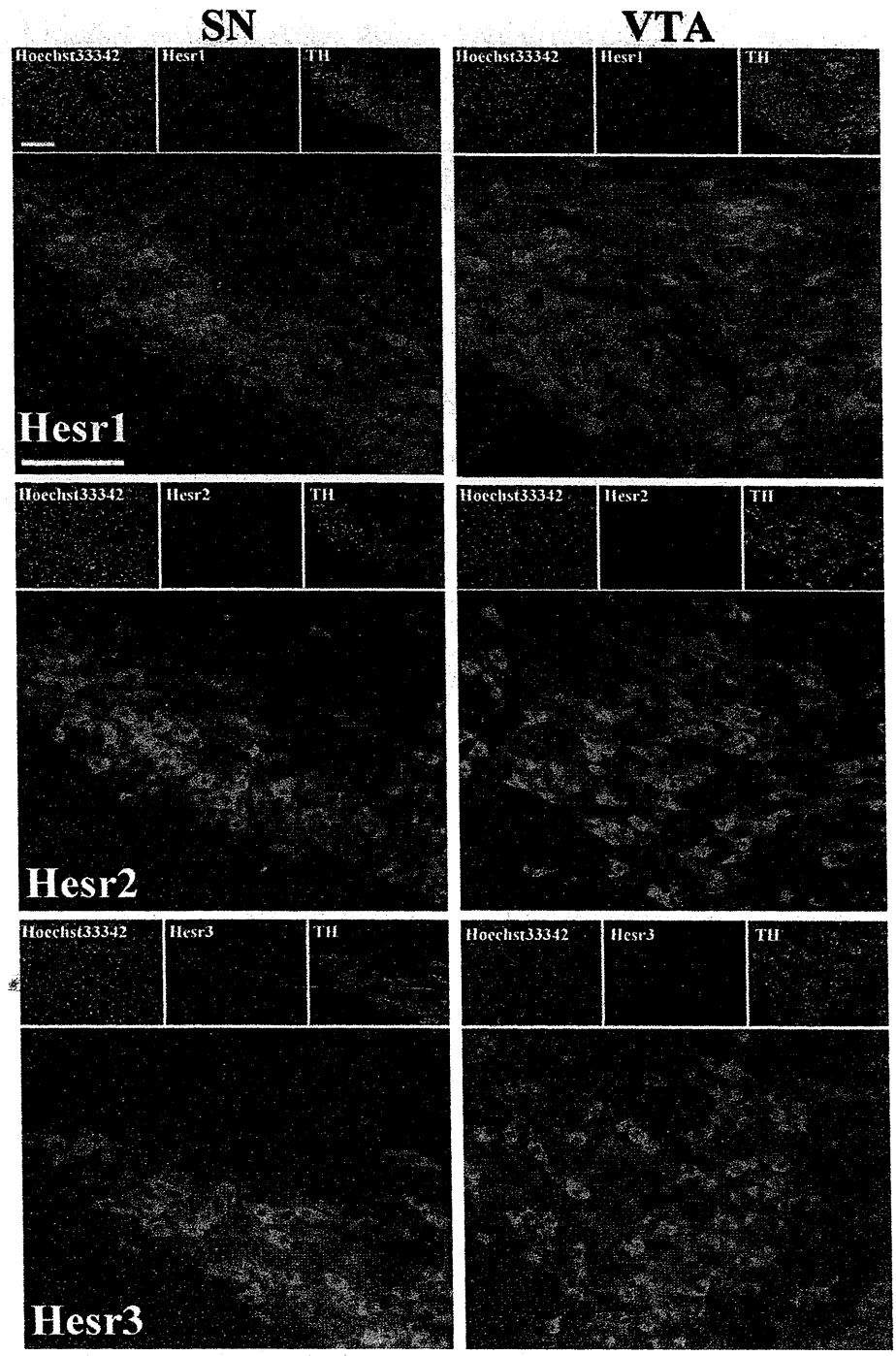

Fig. 8. Colocalization of Hesr family proteins with dopaminergic neurons. Fluorescence immunohistochemical analysis of the Hesr family protein and tyrosine hydroxylase (TH) distribution in the substantia nigra (SN) and ventral tegmental area (VTA). Hesr, magenta (Cy3); TH, green (Cy2); Hoechst 33342, blue. Scale bars = 100 μm.

family, or at least HESR1 and -2, differentially alter *DAT1* expression depending on the VNTR allele. This supports our idea that cell-specific factors regulate *DAT1* expression in a VNTR allele-specific manner and may explain the discrepancies among previous studies (D'souza and Craig, 2008).

Functional Considerations

We first reported the functional significance of the *DAT* VNTR sequence at the molecular level using luciferase reporter assays (Fuke et al., 2001). After our report, other groups reported interesting but conflicting in vitro results (Fuke et al., 2001, 2005; Inoue-Murayama et al., 2002; Miller and Madras, 2002; Greenwood and Kelsoe, 2003; VanNess et al., 2005; Mill et al., 2005; D'souza and Craig, 2008). One explanation for this is that different promoters and cell lines were used in each study. In fact, our previous study (Fuke et al., 2005) revealed that the inhibitory effect of the *DAT* 3′-UTR in CP-Luc/exon15 was not detected in HEK293 cells, but we could detected it in SH-SY5Y, Neuro2A, and COS-7 cell lines. Every cell line might not express all the transcription factors necessary for regulation of the *DAT1* gene, as D'souza and Craig (2008) speculated. Thus, the identification of the regulating factor for *DAT1* was necessary. We previously identified HESR1 as a 3′-UTR-binding protein using a yeast one-hybrid system (Fuke et al., 2005) and showed that HESR1 inhibited the luciferase activity of CP-Luc/exon 15 in SY-SY5Y, Neuro2A, COS-7, and also HEK293 cells. This indicates that HESR1 may regulate *DAT1* expression.

We also reported the increased expression of *DAT* in the brains of *Hesr1* KO mice. These mice also showed a decrease in spontaneous locomotor activity and a reduction in exploration of novelty (Fuke et al., 2006). This is consistent with our previous and present results, insofar as HESR1 is thought to be a *DAT*-inhibitory factor. In addition, the expression of several dopamine receptor genes (*DRD1*, *DRD2*, *DRD4*, and *DRD5*), the main targets of synaptic dopamine responsiveness, were enhanced in *Hesr1* KO mice. These phenomena are in contrast to what is seen in *DAT* KO mice. Mice lacking *DAT* show decreased intraneural dopamine storage and spontaneous hyperlocomotion following the down-regulation of several dopamine-related genes, including those encoding dopamine receptors D1 and D2 (Giros et al., 1996; Caine, 1998; Jaber et al., 1999; Fauchey et al., 2000; Gainetdinov et al., 2002). This result highlights the importance of Hesr1 in the dopaminergic system in vivo and suggests that further investigation of the in vivo functions of Hesr2 and -3 is needed.

The *Hesr1/2* double mutation is known to be embryonic lethal as a result of cardiac and vascular dysplasia, and both genes have been shown to be involved in neural development (Sakamoto et al., 2003; Fischer et al., 2004; Kokubo et al., 2005). However, whereas *Hesr2* KO mice exhibited heart dysfunction (Kokubo et al., 2004), *Hesr1* KO mice exhibited no obvious morphological or anatomical phenotype (Fischer et al., 2004; Kokubo et al., 2005). On the other hand, interactions between *Hesr1* and transforming growth factor-β (TGF-β) or bone morphogenetic protein (BMP) signaling (Dahlqvist et al., 2003; Takizawa et al., 2003; Zavadil et al., 2004), which functions in the differentiation and maintenance of the dopaminergic nervous system, have been reported (Stull et al., 2001; Farkas et al., 2003; Sanchez-Capelo et al., 2003). *HESR1* may play important roles in the dopaminergic nervous system and the regulation of *DAT*. *HESR* family genes encode a bHLH domain that is essential for DNA binding, an Orange domain and YRPW motif. HESR proteins dimerize with other bHLH proteins via the bHLH domain and bind to corepressors via the YRPW motif (Fischer and Gessler, 2007). Additional investigations are needed to characterize these interacting proteins. In the present study, the results obtained for HESR3 sometimes differed from those obtained for HESR1 and -2. One possible reason for this is the lack of a YRPW motif in HESR3 (Fig. 2).

Our findings may lead to novel therapies for DAT-related disorders. In the case of SERT, YB-1 and CTCF act as regulators of SERT (Klenova et al., 2004) and are targeted by lithium chloride, a mood stabilizer that modifies CTCF and YB-1 expression (Roberts et al., 2007).

DAT gene is expressed exclusively in the dopaminergic neurons (Uhl, 2003). If Hesr family genes are not expressed in the dopaminergic neurons, Hesrs cannot inhibit *DAT* expression via 3′-UTR of DAT. However, as shown in Figures 7 and 8, each Hesr was expressed in dopaminergic neurons throughout the SN and VTA. This suggests that the HESR family influences *DAT* expression in vivo, as observed in our present culture studies. At the same time, these data suggest that HESR family members are involved in mesostriatal and mesocorticolimbic dopamine systems underlying motor control, emotion, and cognition (Bjorklund and Dunnett, 2007).

In a study of prostate cancer, HESR1 was reported to be an androgen receptor-interacting factor (Belandia et al., 2005). It has also been shown that HESR1 is excluded from the nucleus in most human prostate cancers, raising the possibility that abnormal HESR1 subcellular distribution plays a role in the aberrant hormonal responses observed in prostate cancer. In the present study, as shown in Figure 7c, Hesr1 and -2 were localized not only to the nucleus but also to the cytoplasm of nondopaminergic cells in the brain. Thus, the cellular localization of HESR family members may be important for some physiological functions or pathological conditions and warrants further study.

Although it seems clear that the VNTR domain plays a role in regulating *DAT* expression in vitro, there are discrepancies in the proposed differential effects of the various alleles. In vivo studies using transgenic mice with *DAT-9r* or *10r* knock-ins may facilitate the characterization of the mechanisms underlying *DAT* transcriptional regulation. The mouse Hesr data presented here will serve as a molecular basis for generating these animals.

In conclusion, we have demonstrated the differential expression of a luciferase reporter vector containing the *DAT1* 3′-UTR and VNTR domain as well as the differential inhibitory effects of HESR family members on *DAT1* expression via the VNTR domain. Given these findings, additional behavioral and psychiatric studies of personality should be conducted.

ACKNOWLEDGMENTS

We thank Dr. H. Kokubo (National Institute of Genetics) for kindly providing the mouse Hesr constructs and Dr. M.J. Bannon (Wayne State University) for kindly providing us with the DAT1-8317 plasmid. We also thank our former colleagues S. Fuke (RIKEN BSI), O.-A. Asami (University of California, Los Angeles), and K. Toriumi (Meijo University) for technical advice and encouragement. We thank Dr. S. Tsukahara (Saitama University), A. Ito (University of Tokyo), S. Yamada (Kyoto Prefectural University of Medicine), and H. Ito (Weseda University) for technical advice regarding immunohistochemistry. The authors declare no conflict of interest.

REFERENCES

Bannon MJ, Michelhaugh SK, Wang J, Sacchetti P. 2001. The human dopamine transporter gene: gene organization, transcriptional regulation, and potential involvement in neuropsychiatric disorders. Eur Neuropsychopharmacol 11:449–455.

Belandia B, Powell SM, Garcia-Pedrero JM, Walker MM, Bevan CL, Parker MG. 2005. Hey1, a mediator of notch signaling, is an androgen receptor corepressor. Mol Cell Biol 25:1425–1436.

Bjorklund A, Dunnett SB. 2007. Dopamine neuron systems in the brain: an update. Trends Neurosci 30:194–202.

Brookes KJ, Neale BM, Sugden K, Khan N, Asherson P, D'souza UM. 2007. Relationship between VNTR Polymorphisms of the human dopamine transporter gene and expression in post-mortem midbrain tissue. Am J Med Genet B Neuropsychiatr Genet 144B:1070–1078.

Brunswick DJ, Amsterdam JD, Mozley PD, Newberg A. 2003. Greater availability of brain dopamine transporters in major depression shown by Tc-^{99}m TRODAT-1 SPECT imaging. Am J Psychiatry 160:1836–1841.

Caine SB. 1998. Cocaine abuse: hard knocks for the dopamine hypothesis? Nat Neurosci 1:90–92.

Cook EH, Stein MA, Krasowski MD, Cox NJ, Olkon DM, Kieffer JE, Leventhal BL. 1995. Association of attention-deficit disorder and dopamine transporter gene. Am J Hum Genet 56:993–998.

D'souza UM, Craig IW. 2008. Functional genetic polymorphisms in serotonin and dopamine gene systems and their significance in behavioural disorders. Prog Brain Res 172:73–98.

Dahlqvist C, Blokzijl A, Chapman G, Falk A, Dannaeus K, Ibanez CF, Lendahl U. 2003. Functional notch signaling is required for BMP4-induced inhibition of myogenic differentiation. Development 130:6089–6099.

Farkas LM, Dunker N, Roussa E, Unsicker K, Krieglstein K. 2003. Transforming growth factor-beta s are essential for the development of midbrain dopaminergic neurons in vitro and in vivo. J Neurosci 23:5178–5186.

Fauchey V, Jaber M, Caron MG, Bloch B, Le Moine C. 2000. Differential regulation of the dopamine D1, D2 and D3 receptor gene expression and changes in the phenotype of the striatal neurons in mice lacking the dopamine transporter. Eur J Neurosci 12:19–26.

Fischer A, Gessler M. 2007. Delta-Notch-and then? Protein interactions and proposed modes of repression by Hes and Hey bHLH factors. Nucleic Acids Res 35:4583–4596.

Fischer A, Schumacher N, Maier M, Sendtner M, Gessler M. 2004. The Notch target genes Hey1 and Hey2 are required for embryonic vascular development. Gene Dev 18:901–911.

Franklin KBJ, Paxinos G. 2008. The mouse brain in stereotaxic coordinates. Amsterdam: Elsevier/Academic Press.

Fuke S, Suo S, Takahashi N, Koike H, Sasagawa N, Ishiura S. 2001. The VNTR polymorphism of the human dopamine transporter (*DAT1*) gene affects gene expression. Pharmacogenomics J 1:152–156.

Fuke S, Sasagawa N, Ishiura S. 2005. Identification and characterization of the Hesr1/Hey1 as a candidate trans-acting factor on gene expression through the 3′ non-coding polymorphic region of the human dopamine transporter (*DAT1*) gene. J Biochem 137:205–216.

Fuke S, Minami N, Kokubo H, Yoshikawa A, Yasumatsu H, Sasagawa N, Saga Y, Tsukahara T, Ishiura S. 2006. Hesr1 knockout mice exhibit behavioral alterations through the dopaminergic nervous system. J Neurosci Res 84:1555–1563.

Gainetdinov RR, Sotnikova TD, Caron MG. 2002. Monoamine transporter pharmacology and mutant mice. Trends Pharmacol Sci 23:367–373.

Giros B, Caron MG. 1993. Molecular characterization of the dopamine transporter. Trends Pharmacol Sci 14:43–49.

Giros B, Elmestikawy S, Bertrand L, Caron MG. 1991. Cloning and functional characterization of a cocaine-sensitive dopamine transporter. FEBS Lett 295:149–154.

Giros B, Elmestikawy S, Godinot N, Zheng KQ, Han H, Yangfeng T, Caron MG. 1992. Cloning, pharmacological characterization, and chromosome assignment of the human dopamine transporter. Mol Pharmacol 42:383–390.

Giros B, Jaber M, Jones SR, Wightman RM, Caron MG. 1996. Hyperlocomotion and indifference to cocaine and amphetamine in mice lacking the dopamine transporter. Nature 379:606–612.

Greenwood TA, Kelsoe JR. 2003. Promoter and intronic variants affect the transcriptional regulation of the human dopamine transporter gene. Genomics 82:511–520.

Heinz A, Goldman D, Jones DW, Palmour R, Hommer D, Gorey JG, Lee KS, Linnoila M, Winberger DR. 2000. Genotype influences in vivo dopamine transporter availability in human striatum. Neuropsychopharmacology 22:133–139.

Henderson AM, Wang SJ, Taylor AC, Aitkenhead M, Hughes CCW. 2001. The basic helix-loop-helix transcription factor HESR1 regulates endothelial cell tube formation. J Biol Chem 276:6169–6176.

Inoue-Murayama M, Adachi S, Mishima N, Mitani H, Takenaka O, Terao K, Hayasaka I, Ito S, Murayama Y. 2002. Variation of variable number of tandem repeat sequences in the 3′-untransiated region of primate dopamine transporter genes that affects reporter gene expression. Neurosci Lett 334:206–210.

Iso T, Sartorelli V, Poizat C, Iezzi S, Wu HY, Chung G, Kedes L, Hamamori Y. 2001. HERP, a novel heterodimer partner of HES/E(spl) in notch signaling. Mol Cell Biol 21:6080–6089.

Iso T, Kedes L, Hamamori Y. 2003. HES and HERP families: Multiple effectors of the Notch signaling pathway. J Cell Physiol 194:237–255.

Jaber M, Dumartin B, Sagne C, Haycock JW, Roubert C, Giros B, Bloch B, Caron MG. 1999. Differential regulation of tyrosine hydroxylase in the basal ganglia of mice lacking the dopamine transporter. Eur J Neurosci 11:3499–3511.

Jackson DM, Westlinddanielsson A. 1994. Dopamine receptors: molecular biology, biochemistory and behavioral aspects. Pharmacol Ther 64:291–370.

Jacobsen LK, Staley JK, Zoghbi S, Seibyl JP, Kosten TR, Innis RB, Gelernter J. 2000. Prediction of dopamine transporter binding availability by genotype: a preliminary report. Am J Psychiatry 157:1700–1703.

Kilty JE, Lorang D, Amara SG. 1991. Cloning and expression of a cocaine-sensitive rat dopamine transporter. Science 254:578–579.

Klenova E, Scott AC, Roberts J, Shamsuddin S, Lovejoy EA, Bergmann S, Bubb VJ, Royer HD, Quinn JP. 2004. YB-1 and CTCF differentially regulate the 5-HTT polymorphic intron 2 enhancer which predisposes to a variety of neurological disorders. J Neurosci 24:5966–5973.

Kokubo H, Lun Y, Johnson RL. 1999. Identification and expression of a novel family of bHLH cDNAs related to *Drosophila* hairy and enhancer of split. Biochem Biophys Res Commun 260:459–465.

Kokubo H, Miyagawa-Tomita S, Tomimatsu H, Nakashima Y, Nakazawa M, Saga Y, Johnson RL. 2004. Targeted disruption of hesr2 results in atrioventricular valve anomalies that lead to heart dysfunction. Circ Res 95:540–547.

Kokubo H, Miyagawa-Tomita S, Nakazawa M, Saga Y, Johnson RL. 2005. Mouse hesr1 and hesr2 genes are redundantly required to mediate Notch signaling in the developing cardiovascular system. Dev Biol 278:301–309.

Kokubo H, Tomita-Miyagawa S, Hamada Y, Saga Y. 2007. Hesr1 and Hesr2 regulate atrioventricular boundary formation in the developing heart through the repression of Tbx2. Development 134:747–755.

Kouzmenko AP, Pereira AM, Singh BS. 1997. Intronic sequences are involved in neural targeting of human dopamine transporter gene expression. Biochem Biophys Res Commun 240:807–811.

Krause KH, Dresel SH, Krause J, la Fougere C, Ackenheil M. 2003. The dopamine transporter and neuroimaging in attention deficit hyperactivity disorder. Neurosci Biobehav Rev 27:605–613.

Leimeister C, Externbrink A, Klamt B, Gessler M. 1999. Hey genes: a novel subfamily of hairy- and Enhancer of split related genes specifically expressed during mouse embryogenesis. Mech Dev 85:173–177.

Madras BK, Gracz LM, Fahey MA, Elmaleh D, Meltzer PC, Liang AY, Stopa EG, Babich J, Fischman AJ. 1998. Altropane, a SPECT or PET imaging probe for dopamine neurons: III. Human dopamine transporter in postmortem normal and Parkinson's diseased brain. Synapse 29:116–127.

Martinez D, Gelernter J, Abi-Dargham A, van Dyck CH, Kegeles L, Innis RB, Laruelle M. 2001. The variable number of tandem repeats polymorphism of the dopamine transporter gene is not associated with significant change in dopamine transporter phenotype in humans. Neuropsychopharmacology 24:553–560.

Michelhaugh SK, Fiskerstrand C, Lovejoy E, Bannon MJ, Quinn JP. 2001. The dopamine transporter gene (SLC6A3) variable number of tandem repeats domain enhances transcription in dopamine neurons. J Neurochem 79:1033–1038.

Mill J, Asherson P, Browes C, D'souza U, Craig I. 2002. Expression of the dopamine transporter gene is regulated by the 3′ UTR VNTR: evidence from brain and lymphocytes using quantitative RT-PCR. Am J Med Genet B Neuropsychiatr Genet 114B:975–979.

Mill J, Asherson P, Craig I, D'souza UM. 2005. Transient expression analysis of allelic variants of a VNTR in the dopamine transporter gene (*DAT1*). BMC Genet 6.

Miller GM, Madras BK. 2002. Polymorphisms in the 3′-untranslated region of human and monkey dopamine transporter genes affect reporter gene expression. Mol Psychiatry 7:44–55.

Missale C, Nash SR, Robinson SW, Jaber M, Caron MG. 1998. Dopamine receptors: From structure to function. Physiol Rev 78:189–225.

Muller-Vahl KR, Berding G, Brucke T, Kolbe H, Meyer GJ, Hundeshagen H, Dengler R, Knapp WH, Emrich HM. 2000. Dopamine transporter binding in Gilles de la Tourette syndrome. J Neurol 247:514–520.

Nakagawa O, Nakagawa M, Richardson JA, Olson EN, Srivastava D. 1999. HRT1, HRT2, and HRT3: a new subclass of bHLH transcription factors marking specific cardiac, somitic, and pharyngeal arch segments. Dev Biol 216:72–84.

Nakagawa O, McFadden DG, Nakagawa M, Yanagisawa H, Hu TH, Srivastava D, Olson EN. 2000. Members of the HRT family of basic helix-loop-helix proteins act as transcriptional repressors downstream of Notch signaling. Proc Natl Acad Sci U S A 97:13655–13660.

Nakamura Y, Koyama K, Matsushima M. 1998. VNTR (variable number of tandem repeat) sequences as transcriptional, translational, or functional regulators. J Hum Genet 43:149–152.

Ohadi M, Shirazi E, Tehranidoosti M, Moghimi N, Keikhaee MR, Ehssani S, Aghajani A, Najmabadi H. 2006. Attention-deficit/hyperactivity disorder (ADHD) association with the *DAT1* core promoter-67 T allele. Brain Res 1101:1–4.

Ohadi M, Keikhaee MR, Javanbakht A, Sargolzaee MR, Robabeh M, Najmabadi H. 2007. Gender dimorphism in the DAT1–67 T-allele homozygosity and predisposition to bipolar disorder. Brain Res 1144:142–145.

Roberts J, Scott AC, Howard MR, Breen G, Bubb VJ, Klenova E, Quinn JP. 2007. Differential regulation of the serotonin transporter gene by lithium is mediated by transcription factors, CCCTC binding protein and Y-box binding protein 1, through the polymorphic intron 2 variable number tandem repeat. J Neurosci 27:2793–2801.

Sacchetti P, Brownschidle LA, Granneman GJ, Bannon MJ. 1999. Characterization of the 5′-flanking region of the human dopamine transporter gene. Brain Res Mol Brain Res 74:167–174.

Sakamoto M, Hirata H, Ohtsuka T, Bessho Y, Kageyama R. 2003. The basic helix-loop-helix genes Hesr1/Hey1 and Hesr2/Hey2 regulate maintenance of neural precursor cells in the brain. J Biol Chem 278:44808–44815.

Sanchez-Capelo A, Colin P, Guibert B, Biguet NF, Mallet J. 2003. Transforming growth factor beta 1 overexpression in the nigrostriatal system increases the dopaminergic deficit of MPTP mice. Mol Cell Neurosci 23:614–625.

Shibuya N, Kamata M, Suzuki A, Matsumoto Y, Goto K, Otani K. 2009. The-67 A/T promoter polymorphism in the dopamine transporter gene affects personality traits of Japanese healthy females. Behav Brain Res 203:23–26.

Shimada S, Kitayama S, Lin CL, Patel A, Nanthakumar E, Gregor P, Kuhar M, Uhl G. 1991. Cloning and expression of a cocaine-sensitive dopamine transporter complementary DNA. Science 254:576–578.

Steidl C, Leimeister C, Klamt B, Maier M, Nanda I, Dixon M, Clarke R, Schmid M, Gessler M. 2000. Characterization of the human and mouse HEY1, HEY2, and HEYL genes: Cloning, mapping, and mutation screening of a new bHLH gene family. Genomics 66:195–203.

Stull ND, Jung JW, Iacovitti L. 2001. Induction of a dopaminergic phenotype in cultured striatal neurons by bone morphogenetic proteins. Brain Res Dev Brain Res 130:91–98.

Takizawa T, Ochiai W, Nakashima K, Taga T. 2003. Enhanced gene activation by Notch and BMP signaling cross-talk. Nucleic Acids Res 31:5723–5731.

Ueno S. 2003. Genetic polymorphisms of serotonin and dopamine transporters in mental disorders. J Med Invest 50:25–31.

Ueno S, Nakamura M, Mikami M, Kondoh K, Ishiguro H, Arinami T, Komiyama T, Mitsushio H, Sano A, Tanabe H. 1999. Identification of a novel polymorphism of the human dopamine transporter (*DAT1*) gene and the significant association with alcoholism. Mol Psychiatry 4:552–557.

Uhl GR. 2003. Dopamine transporter: Basic science and human variation of a key molecule for dopaminergic function, locomotion, and parkinsonism. Mov Disord 18:S71–S80.

Vandenbergh DJ, Persico AM, Hawkins AL, Griffin CA, Li X, Jabs EW, Uhl GR. 1992. Human dopamine transporter gene (*DAT1*) maps to chromosome 5p15.3 and displays a VNTR. Genomics 14:1104–1106.

Vandenbergh DJ, Thompson MD, Cook EH, Bendahhou E, Nguyen T, Krasowski MD, Zarrabian D, Comings D, Sellers EM, Tyndale RF, George SR, O'Dowd BF, Uhl GR. 2000. Human dopamine transporter gene: coding region conservation among normal, Tourette's disorder, alcohol dependence and

attention-deficit hyperactivity disorder populations. Mol Psychiatry 5:283–292.

VanNess SH, Owens MJ, Kilts CD. 2005. The variable number of tandem repeats element in DAT1 regulates in vitro dopamine transporter density. BMC Genet 6:.

Villaronga MA, Lavery DN, Bevan CL, Llanos S, Belandia B. 2010. HEY1 Leu94Met gene polymorphism dramatically modifies its biological functions. Oncogene 29:411–420.

Wang WL, Campos AH, Prince CZ, Mou YS, Pollman MJ. 2002. Coordinate Notch3-hairy-related transcription factor pathway regulation in response to arterial injury—mediator role of platelet-derived growth factor and ERK. J Biol Chem 277:23165–23171.

Zavadil J, Cermak L, Soto-Nieves N, Bottinger EP. 2004. Integration of TGF-beta/Smad and Jagged1/Notch signalling in epithelial-to-mesenchymal transition. EMBO J 23:1155–1165.

THE JOURNAL OF BIOLOGICAL CHEMISTRY VOL. 286, NO. 52, pp. 44569–44575, December 30, 2011

Comparison of Presenilin 1 and Presenilin 2 γ-Secretase Activities Using a Yeast Reconstitution System*[S]

Received for publication, June 8, 2011, and in revised form, October 25, 2011 Published, JBC Papers in Press, November 10, 2011, DOI 10.1074/jbc.M111.270108

Yoji Yonemura[‡], Eugene Futai[‡1], Sosuke Yagishita[‡], Satoshi Suo[‡], Taisuke Tomita[§], Takeshi Iwatsubo[§], and Shoichi Ishiura[‡2]

From the [‡]Department of Life Sciences, Graduate School of Arts and Sciences, University of Tokyo, Tokyo 153-8902, Japan and the [§]Department of Neuropathology and Neuroscience, Graduate School of Pharmaceutical Sciences, University of Tokyo, Tokyo 113-0033, Japan

γ-Secretase is composed of at least four proteins, presenilin (PS), nicastrin (NCT), Aph1, and Pen2. PS is the catalytic subunit of the γ-secretase complex, having aspartic protease activity. PS has two homologs, namely, PS1 and PS2. To compare the activity of these complexes containing different PSs, we reconstituted them in yeast, which lacks γ-secretase homologs. Yeast cells were transformed with PS1 or PS2, NCT, Pen2, Aph1, and artificial substrate C55-Gal4p. After substrate cleavage, Gal4p translocates to the nucleus and activates transcription of the reporter genes *ADE2*, *HIS3*, and *lacZ*. γ-Secretase activity was measured based on yeast growth on selective media and β-galactosidase activity. PS1 γ-secretase was ~24-fold more active than PS2 γ-secretase in the β-galactosidase assay. Using yeast microsomes containing γ-secretase and C55, we compared the concentration of Aβ generated by PS1 or PS2 γ-secretase. PS1 γ-secretase produced ~24-fold more Aβ than PS2 γ-secretase. We found the optimal pH of Aβ production by PS2 to be 7.0, as for PS1, and that the PS2 complex included immature NCT, unlike the PS1 complex, which included mature NCT. In this study, we compared the activity of PS1 or PS2 per one γ-secretase complex. Co-immunoprecipitation experiments using yeast microsomes showed that PS1 concentrations in the γ-secretase complex were ~28 times higher than that of PS2. Our data suggest that the PS1 complex is only marginally less active than the PS2 complex in Aβ production.

γ-Secretase consists of at least four subunits, presenilin (PS),[3] nicastrin (NCT), anterior pharynx defective 1 (Aph1), and presenilin enhancer 2 (Pen2) (1). PS is the catalytic subunit of γ-secretase with aspartic protease activity (2, 3). Amyloid-β (Aβ) peptide, which plays a causative role in Alzheimer disease (AD), is produced after sequential cleavage of amyloid-β precursor protein (APP) by β-secretase and γ-secretase. The Aβ mainly consists of Aβ40 and Aβ42 containing 40 and 42 amino acids, respectively. Aβ42 is more prone to aggregation (4) and more toxic to neuronal cells. Many studies have reported that familial AD (FAD) mutations in PS and APP result in increased ratios of Aβ42 to Aβ40. The high Aβ42 ratio is believed to lead to AD.

PS has two homologs, namely, PS1 and PS2 (67% identical at the amino acid level). Aph1 also has two homologs: Aph1a (with alternative splicing variants Aph1a-S and a-L) and Aph1b. Sato *et al.* (5) reported that γ-secretase contained only one of each subunit, and as such, six distinct γ-secretases exist. Indeed, both PS1 and PS2 form a γ-secretase complex with the other subunits, producing Aβ (6). γ-Secretase cleaves many type I transmembrane proteins including APP and Notch, but the mechanism by which the different γ-secretases select their substrates is unclear. These different γ-secretases may have different functions and substrate selectivity.

Ubiquitous expression of PS1 and PS2 mRNAs in many human and mouse tissues has been reported, with varying expression levels across their tissues and during brain development (7). For example, in human young adult and aged brains, PS1 and PS2 mRNAs expression was similar. The subcellular distribution of PSs are known to be predominantly in the endoplasmic reticulum and the Golgi compartment (8). Levitan *et al.* (9) showed that human PS1 and PS2 substituted for *Caenorhabditis elegans* sel-12, suggesting that PS1 and PS2 are functionally redundant.

Different phenotypes of PS1- and PS2-deficient mice have been reported. PS1 knock-out mice exhibit severe developmental defects and perinatal lethality (10, 11), whereas PS2 knock-out mice show only mild phenotypes (12). Over 160 FAD mutations in PS1, but only 10 in PS2, have been found. These findings suggest that PS1 and PS2 play distinct roles *in vivo*.

Lai *et al.* (13) indicated that Ps1 (Ps, mouse presenilin) γ-secretase produced 169 times more Aβ than Ps2 γ-secretase, using membrane fractions from Ps1-(+/−), Ps2-(−/−), and Ps1-(−/−), Ps2-(+/+) blastocyst-derived cells from knock-out mice. In their study, γ-secretase activity was calculated as follows: level of produced Aβ/total Ps. They did not use the calculation: level of produced Aβ/Ps in γ-secretase complex and thus did not evaluate the active γ-secretase content.

Yagishita *et al.* (14) developed a novel γ-secretase assay using yeast microsomes. Yeast lacks endogenous γ-secretase and

* This work was supported in part by grants from Human Frontier Science Program and The Ministry of Health, Labor and Welfare, Japan.
[S] The on-line version of this article (available at http://www.jbc.org) contains supplemental Fig. S1.
[1] Present address: Dept. of Molecular and Cell Biology, Graduate School of Agricultural Science, Tohoku University, Sendai, Miyagi 981-8555, Japan.
[2] To whom correspondence should be addressed: 3-8-1 Komaba, Meguro-ku, Tokyo 153-8902, Japan. Tel. and Fax: 81-3-5454-6739; E-mail: cishiura@mail.ecc.u-tokyo.ac.jp.
[3] The abbreviations used are: PS, presenilin; APP, amyloid precursor protein; Aβ, amyloid β peptide; Aph1, anterior pharynx 1; CHAPSO, 3-[(3-cholamidopropyl)dimethylammonio]-2-hydroxy-1-propanesulfonic acid; CTF, carboxyl-terminal fragment; NCT, nicastrin; NTF, amino-terminal fragment; PC, phosphatidyl choline; Pen2, presenilin enhancer 2; FAD, familial Alzheimer disease; TM, transmembrane domain.

APP homologs, and one can reconstitute pure human γ-secretase in yeast and estimate the activity. Using this system, we compared the activity of PS1 and PS2 in γ-secretase complexes. Our data suggested that PS1-containing microsomes had much higher activity than PS2-containing microsomes. However, detailed analysis regarding the "active" γ-secretase complex revealed that the PS1 and PS2 complex produced similar levels of Aβ.

MATERIALS AND METHODS

Construction of γ-Secretase and Substrates—To reconstitute γ-secretase in yeast, human PS1 or PS2, NCT, Aph1a-L-HA, FLAG-Pen2, and substrates were cloned into the following vectors, as described previously (15). Briefly, PS1 or PS2 and NCT were ligated into KpnI and XbaI sites of the pBEVY-T vector (16). Aph1a-L-HA and FLAG-Pen2 were ligated into the XbaI and KpnI sites of pBEVY-L (16). C55-Gal4p, NotchTM-Gal4p, and C99 were fused to the *SUC2* signal sequence, facilitating translocation to the endoplasmic reticulum, and ligated into the BamHI and EcoRI sites of p426ADH (17). C55, C99, and NotchTM indicate amino acids 672–726 of the human APP770 isoform, 672–770 of the human APP770, 1703–1754 of the mouse Notch-1, respectively.

Myc-tagged PS1 and PS2 were PCR amplified and ligated into the KpnI site of pBEVY-T, using the following two pair of primers, respectively: mycPS1S, 5′-GGGGTACCAAAAATGGAACAAAAACTCATCTCAGAAGAGGATCTGATGACAGAGTTACCTGCACCGTTG-3′ and PS1AS, 5′-GATCCGCTTATTTAGAAGTGTCGAATTCGACCTCGGTACCATGCTAGATATAAAATTGATGGAATGC-3′; mycPS2S, 5′-GGGGTACCAAAAATGGAACAAAAACTCATCTCAGAAGAGGATCTGATGCTCACATTCATGGCCTCTGAC-3′ and PS2AS, 5′-GGGGTACCTCAGATGTAGAGCTGATGGGAGG-3′.

Yeast Transformation—Three plasmids were transformed into *Saccharomyces cerevisiae* strain PJ69-4A (*MATa, trp1-901, leu2-3, 112, ura3-52, his3-200, gal4Δ, gal80Δ, LYS2::GAL1-HIS3, GAL2-ADE2, met2::GAL7-lacZ*) (18). The transformants were selected on SD media plate lacking Leu, Trp, and Ura (SD-LWU). In microsome assays, we used the yeast strain PJ69-4Apep4Δ(*MATa, trp1-901, leu2-3, 112, ura3-52, his3-200, gal4Δ, gal80Δ, LYS2::-GAL1-HIS3, GAL2-ADE2, met2::GAL7-lacZ, pep4::kanMX*) (14) to avoid endogenous protease activity.

Reporter Gene Expression—Expression of *HIS3* (His) and *ADE2* (Ade) was estimated by transformant growth on SD-LWHUAde. β-Galactosidase assays were performed as described previously (15). Transformants were cultured in SD-LWU media until they reached an A_{600} of ~0.8. Cells were collected after centrifugation and suspended in lysis buffer (20 mM Tris-Cl (pH 8.0), 10 mM $MgCl_2$, 50 mM KCl, 1 mM EDTA, 5% glycerol, 1 mM dithiothreitol) including protease inhibitor mixture (Sigma), and lysed by glass beads. Protein concentration and β-galactosidase activity of the cell lysates were determined.

γ-Secretase Assay and Immunoblotting—Using yeast microsomes, we detected Aβ using an in vitro γ-secretase assay. *In vitro* γ-secretase assays were performed as described previously, with minor modifications (14). Microsomes (80 μg) were solubilized with γ-buffer (50 mM MES (pH 5.5) or 50 mM PIPES (pH 6.0, 6.5, 7.0, 7.5), or 50 mM HEPES (pH 8.0), 250 mM sucrose, 1 mM EGTA) containing 1% CHAPSO on ice for 60 min. Inhibitor mixture, thiorphan, *O*-phenanthroline, CHAPSO, and γ-buffer were added to the solubilized microsomes, as described previously (14). The mixture was incubated at 37 °C for 0 or 24 h. After incubation, the sample was extracted with chloroform/methanol (2:1) followed by addition of sample buffer, and boiled at 100 °C for 5 min. Aβ production was analyzed by Western blotting using the specific antibody, 82E1. Band signal was quantified using an LAS-3000 luminescent image analyzer (FujiFilm, Tokyo, Japan).

Immunoprecipitation of γ-Secretase—Microsomes (400 μg) were solubilized with IP buffer containing 1% CHAPSO and protease inhibitor mixture, on ice, for 60 min. Solubilized membranes were added to 40 μl of anti-FLAG affinity gel (50% slurry) (Sigma) and rotated at 4 °C for 2 h. Beads were washed with IP buffer and suspended in sample buffer containing 8 M urea to prepare the "IP sample" from 400 μg of microsomes. The "input sample" was prepared as follows: 100 μl of sample buffer containing 8 M urea was added to 80 μg of microsomes and incubated at 65 °C for 10 min. Microsomes (8 μg, 10–11 μl) were loaded as input.

Antibodies—The following antibodies were used for immunoblotting: monoclonal antibodies against Aβ, 82E1 (IBL, Fujioka, Japan), HA (12CA5; Sigma), FLAG (M2; Sigma), and polyclonal antibodies against NCT (AB5890; Chemicon, Temecula, CA), Myc, 2272 (Cell Signaling Technology, Beverly, MA), the PS1 loop region (G1L3) (19), and the PS2 loop region (G2L) (20).

RESULTS

PS2 Was Less Active than PS1 in Growth and β-Galactosidase Assays—We constructed recombinant plasmids for γ-secretase and APP-based (C55-Gal4p) or Notch-based substrates (NotchTM-Gal4p) (15). We introduced the vectors into yeast strain PJ69, which expresses *HIS3*, *ADE2*, and *lacZ* under Gal4p control, and generated yeast transformants expressing the γ-secretase subunits (PS1 or PS2, NCT, Aph1a-L-HA, FLAG-Pen2) and an artificial substrate (C55-Gal4p or NotchTM-Gal4p). Gal4p released from C55-Gal4p or NotchTM-Gal4p by reconstituted γ-secretase activates *HIS3* and *ADE2* genes transcription. Therefore, γ-secretase activity was assessed by growth on media lacking histidine and adenine. As a result, yeast expressing PS1 γ-secretase and C55-Gal4p could replicate on the selection media. Yeast expressing PS2 γ-secretase could also grow, but was much slower than that of PS1-expressing yeast (Fig. 1*A*). PS1 L166P, G384A, and PS2 N141I are familial Alzheimer disease (FAD) mutations. Yeast carrying these mutations were unable to grow on media lacking histidine and adenine. After isolating these yeast cell lysates, we measured β-galactosidase activity to estimate γ-secretase activity. PS1 had ~24 times more β-galactosidase activity than PS2 (Fig. 1*B*). The results of the β-galactosidase assay were well correlated with the growth assay results (Fig. 1, *A* and *B*).

Next, we used NotchTM-Gal4p as a substrate instead of C55-Gal4p. The results were similar to those obtained when using

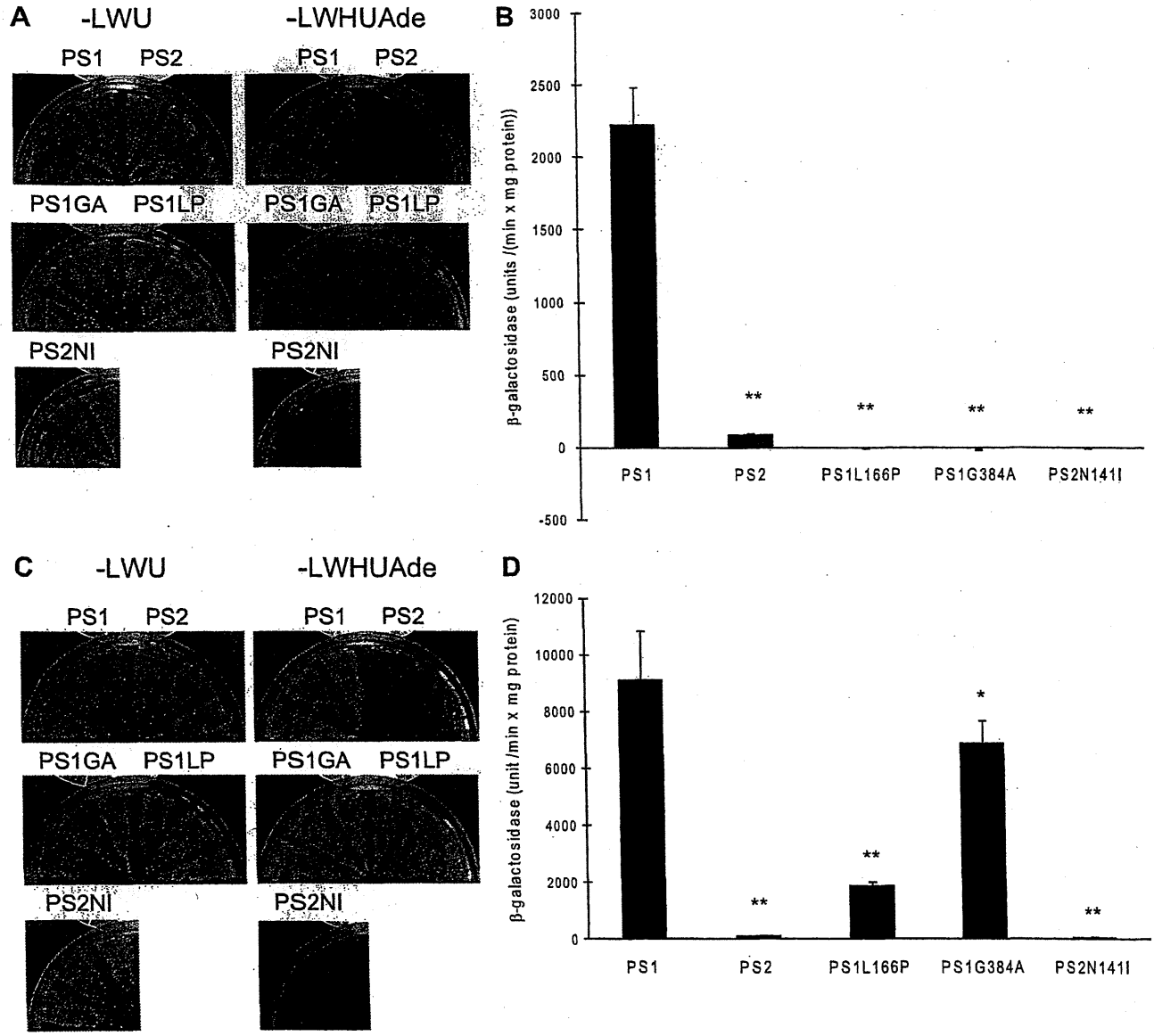

FIGURE 1. **Estimate of reconstituted PS1 or PS2 γ-secretase activity in yeast.** *A* and *C*, yeast cells were transformed with PSs (PS1 or PS2, or PS with FAD mutations), NCT, FLAG-Pen2, Aph1a-L-HA, and C55-gal4p (*A*), or NotchTM-gal4p (*C*). Three independent clones were cultured on non-selection media (SD-LWU) or selection media (SD-LWHUAde) at 30 °C for 3 days. Yeast cells not expressing PS did not grow on SD-LWHUAde. *B* and *D*, β-galactosidase activity was measured for each yeast lysate. Lysates were prepared from yeast cells using glass beads. One unit of β-galactosidase activity corresponds to 1 nmol of *O*-nitrophenyl β-d-galactopyranoside hydrolyzed per min, and activity was calculated as unit/(min × mg of protein in lysate). The activity was normalized by subtracting the activity in the absence of PS, 65 unit/(min × mg protein). Data are presented as mean value ± S.D., $n = 18$ (*A*), $n = 3$ (*C*) *, $p < 0.05$; **, $p < 0.01$ (analyzed by one-way analysis of variance followed by Dunnett's multiple comparison test). Statistical analyses were performed with PRISM software.

the C55-Gal4p, with the following two exceptions. Notch1 was more likely to be cleaved by γ-secretase than C55 (APP) (Fig. 1, *B versus D*) and yeast cells expressing PS1 with FAD mutations (L166P and G384A) were able to grow on SD-LWHUAde, whereas cells expressing PS2 N141I were not (Fig. 1*D*). These results suggested that PS1 with the FAD mutations cannot cleave APP, whereas they can cleave Notch like wild-type γ-secretase.

Optimal pH for Aβ Production by the PS2 Complex—To study γ-secretase activity *in vitro*, we prepared yeast microsomes from yeast transformants expressing PS1 or PS2, NCT, Aph1a-L-HA, FLAG-Pen2, and C55 (14). Three previous reports showed that γ-secretase with PS1 maximally produced Aβ at approximately pH 7.0 (14, 21, 22). The optimum pH of Aβ production by γ-secretase with PS2, however, remains unclear. Thus, we investigated the optimal pH of the PS2 complex to produce Aβ. When yeast microsomes prepared from three independent clones were incubated for 24 h at 37 °C with 0.25% CHAPSO and 0.1% PC, we found that the PS2 complex also maximally produced Aβ at approximately pH 7.0 in all three assays (Fig. 2, *A* and *B*), suggesting that the PS1 and PS2 complex have similar pH dependences for Aβ production.

Levels of Aβ Production by PS1 or PS2—We compared the level of Aβ produced by PS1 or PS2 using yeast microsomes. Each microsome was incubated at 37 °C for 24 h in the pres-

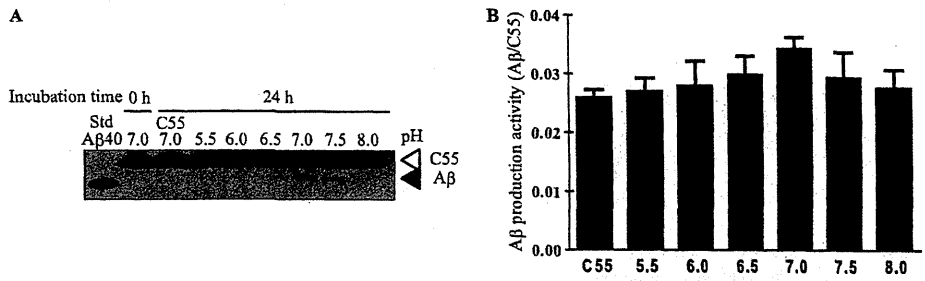

FIGURE 2. **Optimum pH of Aβ production by PS2.** *A*, microsomes (80 μg) prepared from three independent yeast cells transformed with PS2, NCT, Aph1a-L-HA, FLAG-Pen2, and C55, and from yeast expressing C55 were incubated with 0.25% CHAPSO and 0.1% PC at 37 °C for 0 or 24 h. Incubation samples were subjected to immunoblotting to compare Aβ production activity, Aβ/C55. Aβ was detected by 82E1. Synthetic Aβ40 (20 pg) was used as a positive control. Yeast expressing C55 and microsomes incubated for 0 h were loaded as a negative control. *B*, three independent assays were quantified using analyzing software (LAS-3000 luminescent image analyzer, Fuji Film, Tokyo, Japan). The column represents the mean ± S.D. ($n = 3$).

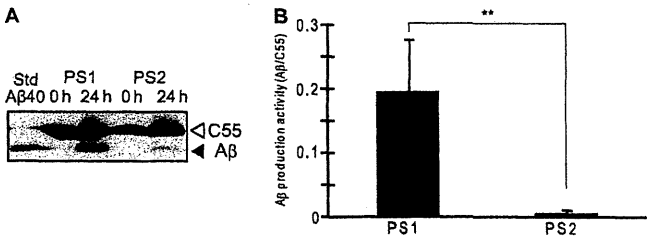

FIGURE 3. **Difference in Aβ production between PS1 and PS2.** *A*, yeast microsomes expressing PS1 or PS2, NCT, Aph1a-L-HA, FLAG-Pen2, and C55 were subjected to *in vitro* γ-secretase assays at pH 7.0. Aβ produced by PS1 or PS2 γ-secretase was detected. Synthetic Aβ40 (30 pg) was loaded as a marker. *B*, the bands obtained in *A* were quantified to determine the ratio of Aβ to C55 using analyzing software (LAS-3000 luminescent image analyzer, Fuji Film, Tokyo, Japan). The column represents the mean ± S.D. ($n = 5$, **, $p < 0.01$). Data were analyzed by Student's *t* test.

ence of 0.25% CHAPSO and 0.1% PC. We found that the PS1 complex produced significantly more Aβ than PS2 (Fig. 3*A*). By quantifying the Western blotting signals, we calculated that PS1 produced ~24 times more Aβ than PS2 (Fig. 3*B*).

PS1 Complexes Were More Abundant than PS2 Complexes—To verify whether PS, NCT, Aph1a-L, and Pen2 form the γ-secretase complex, we isolated membrane fractions from yeast introduced with PS, NCT, Aph1a-L-HA, FLAG-Pen2, and C99, and performed co-immunoprecipitation experiments with the anti-FLAG M2 affinity gel. Both PS1 and PS2 were co-immunoprecipitated with FLAG-Pen2 (Fig. 4, *B* and *C*). NCT and Aph1a-L were also co-immunoprecipitated with FLAG-Pen2 (Fig. 4*A*), suggesting that PS1 and PS2 formed a γ-secretase complex. We also found that the PS2 complex predominantly included non-glycosylated immature NCT, whereas the PS1 complex contained highly glycosylated mature NCT (Fig. 4*A*).

Comparison of the PS1 and PS2 contents in γ-secretase is difficult due to the variable affinity of their specific antibodies. To estimate the amount of PS1 or PS2 in γ-secretase complexes, we constructed Myc-tagged PS1 and PS2. We introduced these constructs into yeast and reconstituted the γ-secretases. Preparing these microsomes, we immunoprecipitated γ-secretase complexes with anti-FLAG affinity gel. The immunoprecipitates were next subjected to immunoblotting. Aph1a-L levels in the PS1 or PS2 complex were similar (Fig. 5*A*). The Myc-tagged PS1 complex included mainly mature NCT, while Myc-tagged PS2 complexes contained immature NCT (Fig. 5*A*). The level of PS1 NTF in γ-secretase complexes (associated with FLAG Pen2) was ~28 times higher than that of PS2 NTF (Fig. 5*B*).

When calculating γ-secretase activity per one γ-secretase complex from these data, a significant difference between PS1 and PS2 does not exist. However, the PS1 complex was 24.15 more active in the β-galactosidase assay. *In vitro* Aβ production assays indicated that PS1 was 24.61 more active than PS2. Comparing PS1 and PS2 contents in γ-secretase in a co-immunoprecipitation experiment, we found that the amount of PS1NTF in the γ-secretase complex was 28.14 times higher than that of PS2NTF. These data suggested that the complete PS2 complex was 1.142 or 1.143 times more active than the PS1 complex.

DISCUSSION

γ-Secretase assays measuring released Aβ into conditioned media from cultured cells have been previously performed. These assays found that γ-secretase with PS FAD mutations increased the Aβ 40/42 ratio. However, very few *in vitro* assays have been reported. To accurately study γ-secretase activity, Yagishita *et al.* (14) established an *in vitro* assay system using yeast, which possesses no γ-secretase homologs. This system enabled us to directly compare activities between the PS1 and PS2 complex.

Yeast growth and β-galactosidase assays using C55-Gal4p or Notch-Gal4p as a substrate revealed that PS1 had a significantly higher activity than PS2. We also found that FAD mutations in PS abolished APP processing activity, and that PS1 L166P and G384A cleaved Notch with reduced activity compared with wild-type PS1. The assembly of PS1 FAD mutants (L166P or G384A) into γ-secretase complex was also assessed by immunoprecipitation (supplemental Fig. S1). The assembly of PS1 L166P mutant was similar to PS1 WT. On the other hand, ~36% of PS1 G384A (comparing to the WT) formed the γ-secretase complex. These results showed that PS1 L166P assembled normally with defective protease activity and PS1 G384A was defective both in the assembly and the protease activity, suggesting that loss of function of PS caused lower cleavage activity. These reductions in processing activity obtained in this report support PS loss of function hypothesis, which is believed to cause FAD (23). We evaluated the activity of other PS1 FAD mutations (A79V, M146L, A231V, M233T, and ΔExon9) in Notch cleavage (data not shown). Our Notch

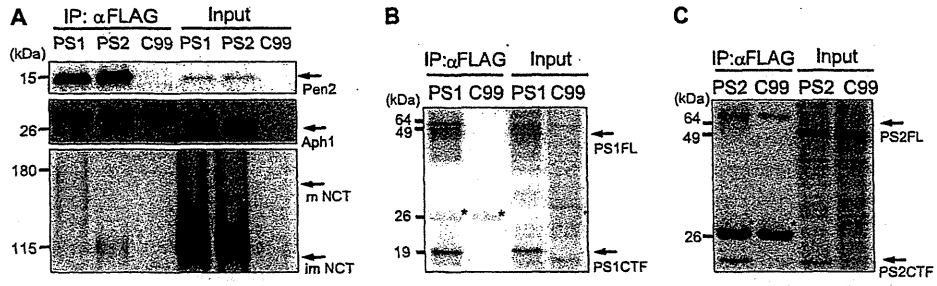

FIGURE 4. **Formation of PS1 and PS2 γ-secretase complexes.** Yeast microsomes expressing PS1 or PS2, NCT, Aph1a-L-HA, FLAG-Pen2, and C99, and microsomes expressing C99 were solubilized with IP buffer containing 1% CHAPSO and protease inhibitor mixture. γ-Secretase complexes were immunoprecipitated with anti-FLAG affinity gel (Sigma). The immunoprecipitates and input fraction were subjected to immunoblotting. NCT, Aph1, Pen2, and PS were detected by specific antibodies. The *asterisks* indicate nonspecific bands.

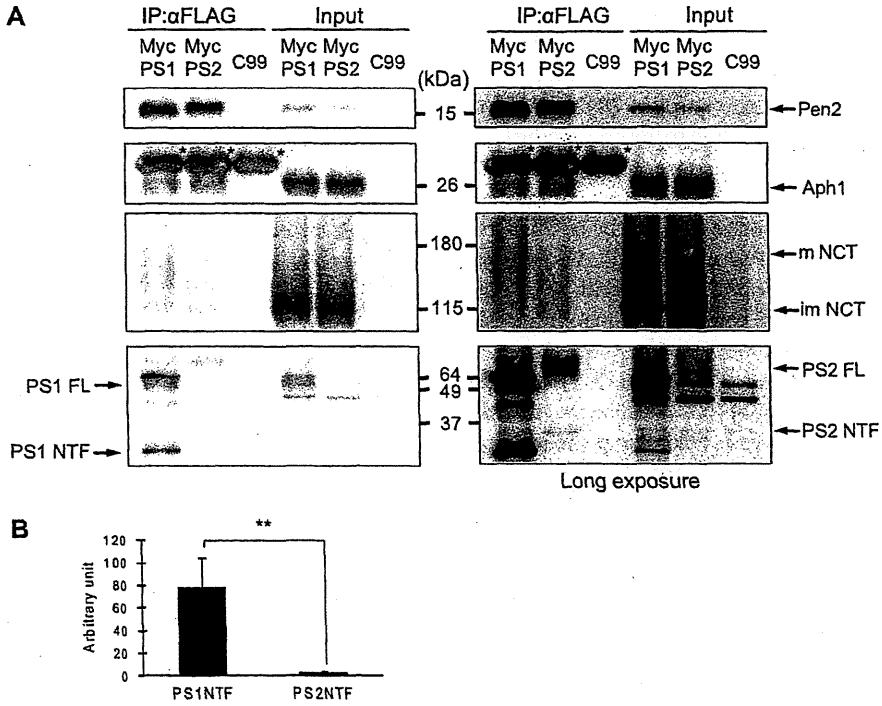

FIGURE 5. **Quantification of PS1 and PS2 in γ-secretase complexes.** *A*, yeast expressing Myc-tagged PS1 or PS2, the other secretase subunits, and C99, were incubated with anti-FLAG affinity gel. The immunoprecipitates were analyzed by immunoblotting. *B*, amount of Myc-tagged PS1NTF and Myc-tagged PS2NTF in the γ-secretase complexes were quantified using LAS-3000 luminescent image analyzer (Fuji Film, Tokyo, Japan). Data were analyzed by Student's *t* test. Error bar shows the mean ± S.D. $n = 4$, **, $p < 0.01$. The *asterisks* indicate nonspecific bands.

cleavage results with PS1 FAD mutations, PS1L166P and G384A, corroborated the findings of earlier studies (24, 25).

Based on the *in vitro* γ-secretase assay using yeast microsomes, we found that γ-secretase with PS2 optimally produced Aβ at approximately pH 7.0. Previous reports have shown that PS1 also maximally produced Aβ at pH 7.0 (14, 21, 22), suggesting that PS1 and PS2 make Aβ using a similar mechanism.

Our co-immunoprecipitation experiments using yeast microsomes containing PS1 or PS2, NCT, Aph1a-L-HA, and FLAG-Pen2 showed that PS2 bound to immature NCT, whereas PS1 bound to the mature NCT. Expression levels of immature or mature NCTs in cells transformed with PS1 or PS2 were similar, but the anti-FLAG affinity gel immunoprecipitates contained different levels of immature and mature NCT. Frånberg *et al.* (26) reported that Ps2 bound to immature NCT in Ps1-deficient (Ps1-(−/−), Ps2-(+/+)) MEF cells and Ps1 bound to mature NCT in Ps2 deficient (Ps1-(+/+), Ps2-(−/−)) MEF cells using affinity capture with an active site-directed γ-secretase inhibitor. This difference in NCT maturation in the complex may affect substrate affinity.

In this study, we used Aph1a-L as a γ-secretase subunit, which may facilitate PS2 binding to immature NCT. Also, Aph1a-S expression, or Aph1b as a γ-secretase subunit, may result in alternative binding patterns, such as PS2 binding to mature NCT or PS1 binding with immature NCT. In fact, we observed the PS1 complex with Aph1a-S containing more immature NCT than the PS1 complex with Aph1a-L (data not shown). To date, γ-secretase is known to target many substrates, but how γ-secretase selects its substrates is unclear. These variable γ-secretases may contribute to specific substrate selection.

To compare the γ-secretase activity of PS1 and PS2 precisely, we employed two different approaches. First, we used C55(-Gal4p) or C99 as a substrate instead of C100Flag. NCT

plays a role in binding to the substrate by recognizing N terminus of C99 (27). So, natural N terminus of C99 or C55 is important to assess γ-secretase activity correctly. Using C100Flag as a substrate may result in inaccurate evaluation, because C100Flag possesses one extra amino acid, methionine, on the N terminus. Second, we estimated the amount of PS1 or PS2 in the γ-secretase complex. Lai *et al.* (13) reported Ps1 and Ps2 γ-secretase activity as a function of total protein concentration, but not all PS localizes to the γ-secretase complex. Therefore, γ-secretase activity should be calculated as follows: γ-secretase activity/concentration of PS in γ-secretase complex. γ-Secretase assembly is not a random process, but occurs sequentially. NCT and Aph1 form the NCT-Aph1 subcomplex in the initial step of complex formation. Two hypotheses have been proposed regarding the subsequent steps in γ-secretase complex assembly. One hypothesis is that PS binds to the NCT-Aph1 subcomplex, followed by Pen2, creating a γ-secretase complex (28, 29). Alternatively, the PS-Pen2 intermediate may bind to the preexisting NCT-Aph1 subcomplex to form the γ-secretase complex (30). To evaluate the construction process of the γ-secretase complex, we compared PS1 or PS2 in the γ-secretase complex by co-immunoprecipitating Myc-tagged PS1 or PS2 with anti-FLAG antibody (FLAG tag is on Pen2). Co-immunoprecipitation with other antibodies detecting NCT, Aph1, or PS could lead to inaccurate estimates regarding the amount of Myc-PS in the γ-secretase complex. We found that the concentration of PS2 in the γ-secretase complex was much lower than that of PS1. Because we applied a minimal reconstitution system in yeast, unknown protein(s) may stabilize PS2. This possibility is currently being explored.

In this study, we reconstituted human PS1 and PS2 γ-secretase complexes and compared their Aβ production (per γ-secretase complex). PS1 had 24.65 times and 24.61 times higher activity than PS2 in the β-galactosidase and *in vitro* Aβ production assay, respectively. Based on Co-IP experiments, the amount of PS1 in the γ-secretase complex was 28.14 times higher than that of PS2. Thus, our data suggest that PS1 did not have significantly higher activity than PS2, as has been reported (13). PS1 and PS2 were 67% identical at the amino acid level, suggesting that these two proteins have related functions in the γ-secretase complex. Our results suggest that the difference between PS1 and PS2 is their affinity to the other γ-secretase subunits. The contribution of PS1 on γ-secretase activity is more important than that of PS2 because PS1 knock-out mice exhibit severe phenotypes, whereas PS2 knock-out mice do not. We hypothesize that the differences in PS1 and PS2 knock-out mice phenotypes may result from different amounts of PS1 and PS2 γ-secretases, but not differences in their activity.

Currently, PS1 is believed to have a higher activity than PS2 in γ-secretases, while we showed that they have similar activities. In corroboration of our findings, recent reports have shown that PS2 γ-secretase cleaved more APP than PS1 γ-secretase in microglia cells, regardless of the presence of PS1 (31). Thus, when studying γ-secretase activity, we should consider the concentration of PS in the active γ-secretase complex, which may aid in clarifying the pathogenesis of FAD caused by PS loss-of-function FAD mutations.

Acknowledgments—We thank Dr. Raphael Kopan for the mNotch1 clone and Dr. Philip James for the PJ-69–4A yeast strain. We also thank the members of our laboratory, especially Yusuke Nagara, Natsumi Ohsawa, and Yuri Watanabe for helpful discussions and technical suggestions.

REFERENCES

1. Edbauer, D., Winkler, E., Regula, J. T., Pesold, B., Steiner, H., and Haass, C. (2003) *Nat. Cell Biol.* **5,** 486–488
2. Wolfe, M. S., Xia, W., Ostaszewski, B. L., Diehl, T. S., Kimberly, W. T., and Selkoe, D. J. (1999) *Nature* **398,** 513–517
3. Steiner, H., Duff, K., Capell, A., Romig, H., Grim, M. G., Lincoln, S., Hardy, J., Yu, X., Picciano, M., Fechteler, K., Citron, M., Kopan, R., Pesold, B., Keck, S., Baader, M., Tomita, T., Iwatsubo, T., Baumeister, R., and Haass, C. (1999) *J. Biol. Chem.* **274,** 28669–28673
4. Jarrett, J. T., and Lansbury, P. T., Jr. (1993) *Cell* **73,** 1055–1058
5. Sato, T., Diehl, T. S., Narayanan, S., Funamoto, S., Ihara, Y., De Strooper, B., Steiner, H., Haass, C., and Wolfe, M. S. (2007) *J. Biol. Chem.* **282,** 33985–33993
6. Shirotani, K., Tomioka, M., Kremmer, E., Haass, C., and Steiner, H. (2007) *Neurobiol. Dis.* **27,** 102–107
7. Lee, M. K., Slunt, H. H., Martin, L. J., Thinakaran, G., Kim, G., Gandy, S. E., Seeger, M., Koo, E., Price, D. L., and Sisodia, S. S. (1996) *J. Neurosci.* **16,** 7513–7525
8. Zhang, J., Kang, D. E., Xia, W., Okochi, M., Mori, H., Selkoe, D. J., and Koo, E. H. (1998) *J. Biol. Chem.* **273,** 12436–12442
9. Levitan, D., Doyle, T. G., Brousseau, D., Lee, M. K., Thinakaran, G., Slunt, H. H., Sisodia, S. S., and Greenwald, I. (1996) *Proc. Natl. Acad. Sci. U.S.A.* **93,** 14940–14944
10. Shen, J., Bronson, R. T., Chen, D. F., Xia, W., Selkoe, D. J., and Tonegawa, S. (1997) *Cell* **89,** 629–639
11. Wong, P. C., Zheng, H., Chen, H., Becher, M. W., Sirinathsinghji, D. J., Trumbauer, M. E., Chen, H. Y., Price, D. L., Van der Ploeg, L. H., and Sisodia, S. S. (1997) *Nature* **387,** 288–292
12. Herreman, A., Hartmann, D., Annaert, W., Saftig, P., Craessaerts, K., Serneels, L., Umans, L., Schrijvers, V., Checler, F., Vanderstichele, H., Baekelandt, V., Dressel, R., Cupers, P., Huylebroeck, D., Zwijsen, A., Van Leuven, F., and De Strooper, B. (1999) *Proc. Natl. Acad. Sci. U.S.A.* **96,** 11872–11877
13. Lai, M. T., Chen, E., Crouthamel, M. C., DiMuzio-Mower, J., Xu, M., Huang, Q., Price, E., Register, R. B., Shi, X. P., Donoviel, D. B., Bernstein, A., Hazuda, D., Gardell, S. J., and Li, Y. M. (2003) *J. Biol. Chem.* **278,** 22475–22481
14. Yagishita, S., Futai, E., and Ishiura, S. (2008) *Biochem. Biophys. Res. Commun.* **377,** 141–145
15. Futai, E., Yagishita, S., and Ishiura, S. (2009) *J. Biol. Chem.* **284,** 13013–13022
16. Miller, C. A., 3rd, Martinat, M. A., and Hyman, L. E. (1998) *Nucleic Acids Res.* **26,** 3577–3583
17. Mumberg, D., Müller, R., and Funk, M. (1995) *Gene* **156,** 119–122
18. James, P., Halladay, J., and Craig, E. A. (1996) *Genetics* **144,** 1425–1436
19. Tomita, T., Takikawa, R., Koyama, A., Morohashi, Y., Takasugi, N., Saido, T. C., Maruyama, K., and Iwatsubo, T. (1999) *J. Neurosci.* **19,** 10627–10634
20. Tomita, T., Tokuhiro, S., Hashimoto, T., Aiba, K., Saido, T. C., Maruyama, K., and Iwatsubo, T. (1998) *J. Biol. Chem.* **273,** 21153–21160
21. Li, Y. M., Lai, M. T., Xu, M., Huang, Q., DiMuzio-Mower, J., Sardana, M. K., Shi, X. P., Yin, K. C., Shafer, J. A., and Gardell, S. J. (2000) *Proc. Natl. Acad. Sci. U.S.A.* **97,** 6138–6143
22. Fraering, P. C., Ye, W., Strub, J. M., Dolios, G., LaVoie, M. J., Ostaszewski, B. L., van Dorsselaer, A., Wang, R., Selkoe, D. J., and Wolfe, M. S. (2004) *Biochemistry* **43,** 9774–9789
23. Shen, J., and Kelleher, R. J., 3rd (2007) *Proc. Natl. Acad. Sci. U.S.A.* **104,** 403–409
24. Steiner, H., Kostka, M., Romig, H., Basset, G., Pesold, B., Hardy, J., Capell, A., Meyn, L., Grim, M. L., Baumeister, R., Fechteler, K., and Haass, C.

(2000) *Nat. Cell Biol.* **2,** 848–851
25. Moehlmann, T., Winkler, E., Xia, X., Edbauer, D., Murrell, J., Capell, A., Kaether, C., Zheng, H., Ghetti, B., Haass, C., and Steiner, H. (2002) *Proc. Natl. Acad. Sci. U.S.A.* **99,** 8025–8030
26. Fränberg, J., Svensson, A. I., Winblad, B., Karlström, H., and Frykman, S. (2011) *Biochem. Biophys. Res. Commun.* **404,** 564–568
27. Shah, S., Lee, S. F., Tabuchi, K., Hao, Y. H., Yu, C., LaPlant, Q., Ball, H., Dann, C. E., 3rd, Südhof, T., and Yu, G. (2005) *Cell* **122,** 435–447
28. LaVoie, M. J., Fraering, P. C., Ostaszewski, B. L., Ye, W., Kimberly, W. T., Wolfe, M. S., and Selkoe, D. J. (2003) *J. Biol. Chem.* **278,** 37213–37222
29. Niimura, M., Isoo, N., Takasugi, N., Tsuruoka, M., Ui-Tei, K., Saigo, K., Morohashi, Y., Tomita, T., and Iwatsubo, T. (2005) *J. Biol. Chem.* **280,** 12967–12975
30. Fraering, P. C., LaVoie, M. J., Ye, W., Ostaszewski, B. L., Kimberly, W. T., Selkoe, D. J., and Wolfe, M. S. (2004) *Biochemistry* **43,** 323–333
31. Jayadev, S., Case, A., Eastman, A. J., Nguyen, H., Pollak, J., Wiley, J. C., Möller, T., Morrison, R. S., and Garden, G. A. (2010) *PloS One* **5,** e15743

The FASEB Journal • Research Communication

An alternative metabolic pathway of amyloid precursor protein C-terminal fragments *via* cathepsin B in a human neuroglioma model

Masashi Asai,[*,†,1,2] Sosuke Yagishita,[‡,2,3] Nobuhisa Iwata,[†,§] Takaomi C. Saido,[†] Shoichi Ishiura,[‡] and Kei Maruyama[*]

[*]Department of Pharmacology, Faculty of Medicine, Saitama Medical University, Saitama, Japan; [†]Laboratory for Proteolytic Neuroscience, RIKEN Brain Science Institute, Saitama, Japan; [‡]Department of Life Sciences, Graduate School of Arts and Sciences, The University of Tokyo, Tokyo, Japan; and [§]Graduate School of Biomedical Sciences, Nagasaki University, Nagasaki, Japan

ABSTRACT **γ-Secretase catalyzes the cleavage of the intramembrane region of the Alzheimer amyloid precursor protein (APP), generating p3, amyloid-β peptide (Aβ), and the APP intracellular domain (AICD). Although a γ-secretase inhibitor has been shown to cause an accumulation of the APP C-terminal fragments (CTFs) α and β and to decrease levels of p3 or Aβ and AICD, we found that treatment with a lysosomotropic weak base, such as chloroquine or ammonium chloride, caused simultaneous accumulation of both CTFs and AICD, suggesting that lysosomal proteases are also involved in processing of APP. This observation was reinforced by the results that cysteine protease inhibitor E-64d and cathepsin B specific inhibitor CA-074Me caused the accumulation of both CTFs and AICD with no change in known secretase activities. γ-Secretase preferentially cleaved phosphorylated CTFs to produce Aβ, but cathepsin B degraded CTFs regardless of phosphorylation. Our results suggest that cathepsin B plays novel roles in the metabolism of APP and that an inhibition of APP phosphorylation is an attractive therapeutic target for Alzheimer's disease.—Asai, M., Yagishita, S., Iwata, N., Saido, T. C., Ishiura, S., Maruyama, K. An alternative metabolic pathway of amyloid precursor protein C-terminal fragments *via* cathepsin B in a human neuroglioma model. *FASEB J.* 25, 3720–3730 (2011). www.fasebj.org**

Key Words: Alzheimer's disease · CA-074Me · γ-secretase · phosphorylation

AMYLOID PRECURSOR PROTEIN (APP) is a type I integral membrane glycoprotein with a single membrane-spanning domain, a large ectoplasmic N-terminal region, and a shorter cytoplasmic C-terminal region (1–3). An understanding of APP metabolism is physiologically and clinically important because APP is a stepwise substrate for β- and γ-secretases in the production of the neurotoxic amyloid-β peptide (Aβ; Aβ40 or Aβ42; refs. 1–4). Thus, β- and γ-secretase inhibitors are pharmacological targets for the treatment or prevention of Alzheimer's disease (AD; refs. 4, 5).

Proteolytic processing of APP has been extensively studied, and two major processing pathways have been described. Initially, α- or β-secretase cleaves APP to produce a secreted N-terminal soluble extracellular fragment of APP (sAPPα or sAPPβ) and membrane-bound C-terminal fragments of APP (CTFα or CTFβ). Sequentially, γ-secretase catalyzes the intramembrane proteolysis of CTFs to produce p3, Aβ, and APP intracellular domain (AICD; refs. 1–4).

Numerous γ-secretase inhibitors have been developed (2, 4, 5), and treatment with a γ-secretase inhibitor causes accumulation of substrates, such as CTFs, and suppression of the production of Aβ and AICD *in vivo* or *in vitro* (6–9). This quantitative balance of CTFs, Aβ, and AICD seems to be dependent on γ-secretase, which is an enzymatic multiprotein complex containing presenilin (PS; either PS1 or PS2) as the active core. However, it has been reported that both CTFs and AICD simultaneously accumulated under treatment with lysosomotropic weak bases, such as chloroquine or ammonium chloride (NH_4Cl; refs. 10, 11). It is highly unlikely that alkalization of the endosome-lysosome system causes γ-secretase dysfunction because γ-secretase can cleave other substrates, such as Notch, and can produce intracellular fragments in the presence of these lysosomal inhibitors. In other words, the accumulation of both products and substrates of γ-secretase is indicative of the presence of proteases other than γ-secretase for the processing of CTFs and AICD.

To identify CTF- and AICD-processing enzymes, we analyzed APP metabolism using a pharmacological

[1] Correspondence: Department of Pharmacology, Faculty of Medicine, Saitama Medical University, 38 Moro-hongo, Moroyama-machi, Iruma-gun, Saitama 350-0495, Japan. E-mail: asai@saitama-med.ac.jp

[2] These authors contributed equally to this work.

[3] Current address: Laboratory for Alzheimer's Disease, RIKEN Brain Science Institute, Saitama, Japan.

doi: 10.1096/fj.11-182154

This article includes supplemental data. Please visit *http://www.fasebj.org* to obtain this information.

0892-6638/11/0025-3720 © FASEB

approach in a human neuroglioma model. We found that cysteine protease inhibitor E-64d (12) and cathepsin B-specific inhibitor CA-074Me (12–15) could cause the accumulation of both CTFs and AICD with no change in α-, β-, and γ-secretase activities. Moreover, we found that γ-secretase prefers phosphorylated CTFs on Thr668 (at a position corresponding to the APP_{695} isoform), whereas cathepsin B catalyzed degradation of CTFs regardless of phosphorylation. Altogether, our results suggest that cathepsin B plays novel roles in the metabolism of the APP C-terminal region and that inhibition of APP phosphorylation is an attractive therapeutic target for AD.

MATERIALS AND METHODS

Reagents

CA-074 (also known as cathepsin B inhibitor III; [L-3-*trans*-(propylcarbamoyl)oxirane-2-carbonyl]-L-isoleucyl-L-proline), CA-074Me (also known as cathepsin B inhibitor IV; [L-3-*trans*-(propylcarbamoyl)oxirane-2-carbonyl]-L-isoleucyl-L-proline methyl ester), E-64d [(L-3-*trans*-ethoxycarbonyloxirane-2-carbonyl)-L-leucine (3-methylbutyl) amide], lactacystine ([*N*-acetyl-*S*-{(2*R*,3*S*,4*R*)-3-hydroxy-2-[(1*S*)-1-hydroxy-2-methylpropyl]-4-methyl-5-oxo-2-pyrrolidinecarbonyl}-L-cysteine), DAPT [also known as γ-secretase inhibitor IX; (3,5-difluorophenylacetyl)-L-alanyl-L-2-phenylglycine *t*-butyl ester], and L-685,458 (also known as γ-secretase inhibitor X; [(2*R*,4*R*,5*S*)-2-benzyl-5-(*t*-butyloxycarbonylamino)-4-hydroxy-6-phenylhexanoyl]-L-leucyl-L-phenylalanine amide) were purchased from the Peptide Institute (Osaka, Japan). β-Secretase inhibitor IV (*N*-[(1*S*, 2*R*)-1-benzyl-3-(cyclopropylamino)-2-hydroxypropyl]-5-[methyl(methylsulfonyl)amino-*N*'-[(1*R*)-1-phenylethyl]isophthalamide), compound E (also known as γ-secretase inhibitor XXI; (*S*,*S*)-2-[2-(3,5-difluorophenyl)-acetylamino]-*N*-(1-methyl-2-oxo-5-phenyl-2,3-dihydro-1H-benzo[e] [1,4]diazepin-3-yl)-propionamide), and cathepsin G inhibitor I ([2-[3-[(1-benzoylpiperidin-4-yl)-methylcarbamoyl] naphthalen-2-yl]-1-naphthalen-1-yl-2-oxoethyl]phosphonic acid) were purchased from Merck KGaA (Darmstadt, Germany). Pepstatin A, chloroquine, and NH_4Cl were obtained from Sigma-Aldrich Co. (St. Louis, MO, USA). Chloroquine was dissolved in sterilized PBS, and all other powdered reagents were dissolved in sterilized dimethyl sulfoxide (DMSO) and added into the cell culture medium to yield 0.2% DMSO as a final concentration.

Cell culture

A murine neuroblastoma Neuro2a (N2a) cell line ($mNotch^{\Delta E}$-N2a cells) stably expressing both mouse Notch-deleted extracellular domain with myc tag ($mNotch^{\Delta E}$) and enhanced green fluorescent protein (16), a human neuroglioma H4 cell line stably expressing human APP_{695} with the Swedish mutation (APP_{NL}-H4 cells) (17) or stably expressing human APP_{695} with the Swedish mutation and a point mutation at a phosphorylation site [Thr to Ala on 668 (APP_{695} numbering); APP_{NL_TA}-H4 cells], and mouse embryonic fibroblast cells with deficiencies of both *PS1* and *PS2* genes ($PS1^{-/-}PS2^{-/-}$ cells) (18) were cultured in DMEM (Invitrogen, Carlsbad, CA, USA) at 37°C in 5% CO_2. The DMEM was supplemented with 10% FBS (Invitrogen), 100 U/ml penicillin, and 100 μg/ml streptomycin (Invitrogen). In addition, G418 (Merck) was supplemented for $mNotch^{\Delta E}$-N2a cells (160 μg/ml) and $PS1^{-/-}PS2^{-/-}$ cells (200 μg/ml), and hygromycin B (Wako Pure Chemicals Industries, Osaka, Japan) was supplemented for APP_{NL}-H4 cells (150 μg/ml) and APP_{NL_TA}-H4 cells (225 μg/ml). After passage by trypsinization, cells were grown for 24–36 h and then treated with reagents: CA-074Me (0.1, 1, or 10 μM), pepstatin A (10 μM), cathepsin G inhibitor I (10 μM), E-64d (10 μM), compound E (1 μM), DAPT (1 μM), L-685,458 (1 μM), β-secretase inhibitor IV (1 μM), lactacystin (1 μM), chloroquine (1 μM), or NH_4Cl (1 mM), for the indicated time.

Sample preparation for Western blot analysis

Cells treated with reagents were harvested and lysed in a buffer containing 10 mM HEPES (pH 7.4), 150 mM NaCl, 0.5% Triton X-100, and protease inhibitor cocktail (Roche Diagnostics, Mannheim, Germany) on ice. The cell lysate was freeze-thawed at three 20-min intervals and centrifuged at 13,000 *g* for 15 min at 4°C. The supernatant protein concentrations were determined using a BCA protein assay kit (Pierce Biotechnology, Rockford, IL, USA). sAPP secreted into the conditioned medium was precipitated with heparin agarose resin (Pierce Biotechnology), as described previously (16).

Western blot analysis

Equal amounts of proteins from the cell lysates or sAPP collected from the equal volumes of the conditioned medium were subjected to SDS-PAGE, and proteins in the gels were transferred to PVDF membranes (Hybond-P; GE Healthcare, Little Chalfont, UK) or nitrocellulose transfer membranes (Protran; Whatman, Dassel, Germany). The membranes were probed with an appropriate primary antibody and then reacted with an appropriate secondary antibody, specifically horseradish peroxidase-conjugated anti-mouse or anti-rabbit IgG (GE Healthcare). The protein band was visualized using an enhanced chemiluminescence (ECL) detection method (GE Healthcare), and band intensity was analyzed with a densitometer (LAS-4000; GE Healthcare), using Science Laboratory 2001 Image Gauge software (GE Healthcare).

Monoclonal antibody 2B3 (Immuno-Biological Laboratories, Gunma, Japan), which recognizes amino acid residues at the C terminus of human sAPPα, was used at a concentration of 2 μg/ml to detect sAPPα (anti-sAPPα antibody). Polyclonal anti-$sAPP\beta_{NL}$ antibody was used at a concentration of 1:1000 to detect $sAPP\beta_{NL}$ (APP with Swedish mutation), as described previously (17). Monoclonal antibody 82E1 (Immuno-Biological Laboratories), which recognizes amino acid residues 1–16 of the human Aβ sequence, was used at a concentration of 1 μg/ml to detect Aβ (anti-Aβ antibody). Polyclonal anti-APP antibody (catalog no. A8717; Sigma-Aldrich), which recognizes amino acid residues 676–695 at the C terminus of the APP_{695} isoform, was used at a concentration of 1:15,000 to detect full-length APP (FL-APP), CTFs, and AICD (anti-APP antibody). Polyclonal anti-phosphorylated APP antibody (Cell Signaling Technology, Danvers, MA, USA), which recognizes the phosphorylation of Thr668, was used at a concentration of 1:1000. Monoclonal antibody AC-74 (Sigma-Aldrich), which recognizes amino acid residues at the N-terminal end of β-actin, was used at a concentration of 1:5000. Monoclonal antibody 9B11 (Cell Signaling Technology), which recognizes the myc epitope tag corresponding to amino acid residues 410–419 of human c-Myc, was used at a concentration of 1:1000.

Cell-free assay

The microsomal fraction was isolated from APP_{NL}-H4 cells, as described previously (8). Briefly, harvested APP_{NL}-H4 cells

were homogenized in buffer A (20 mM PIPES, pH 7.0; 140 mM KCl; 0.25 M sucrose; and 5 mM EGTA), and the homogenates were then centrifuged at 800 *g* for 10 min to remove nuclei and cell debris. The resultant supernatants were centrifuged at 100,000 *g* for 1 h. The pellets were suspended in buffer A and centrifuged again. The resultant pellets were suspended in buffer A containing various protease inhibitors, including 50 μM diisopropyl fluorophosphate (Wako), 50 μM phenylmethylsulfonyl fluoride (Sigma-Aldrich), 0.1 μg/ml N^{α}-*p*-tosyl-L-lysine chloromethyl ketone (Sigma-Aldrich), 0.1 μg/ml antipain (Peptide Institute), 0.1 μg/ml leupeptin (Peptide Institute), 100 μM EGTA (Wako), 1 mM thiorphan (Sigma-Aldrich), and 5 mM phenanthroline (Nacalai Tesque, Kyoto, Japan), for a final concentration of 2.5 mg protein/ml. The mixtures were incubated at 37°C for 1 h with CA-074, CA-074Me, or L-685,458. The reaction was terminated using a solution of chloroform:methanol (2:1). After extracting lipids with chloroform:methanol:water solution (1:2:0.8), the protein fractions were separated on conventional 16.5% Tris/Tricine gels to detect Aβ or AICD product by Western blot analysis.

In vitro degradation assay

In vitro cleavage of AICD was performed in 30 μl of 100 mM sodium acetate buffer (pH 5.5), containing 1 mM EDTA and 8 mM cysteine with or without synthetic AICD (Merck). Various amounts of purified cathepsin B from human liver (Merck) were added with or without 1 μM CA-074. The mixtures were incubated at 37°C for the indicated time, and sample buffer was then added to stop the reaction. The products were analyzed by Western blotting conventional 16.5% Tris/Tricine gels with an anti-APP antibody.

Statistical analysis

All values are expressed as means ± SE. For comparisons of 2 groups, a 2-tailed Student's *t* test was used. For comparisons among >3 groups, a Dunnett's or Student-Newman-Keul multiple comparison test was used. Differences were considered significant at values of $P < 0.05$.

RESULTS

Cathepsin B inhibitors, CA-074Me and E-64d, lead to the accumulation of CTFs and AICD with no change in α- and β-secretase activities

Weak bases, such as chloroquine or NH_4Cl, alkalize the intracellular pH of acidic compartments (19, 20). If there are proteases responsible for the degradation of CTFs and AICD other than γ-secretase, we should be able to detect the accumulation of CTFs by treatment with chloroquine or NH_4Cl in γ-secretase-deficient cells. To verify this hypothesis, we treated *PS1*$^{-/-}$ *PS2*$^{-/-}$ cells and APP_{NL}-H4 cells with chloroquine or NH_4Cl (**Fig. 1*A*, *B***). After chloroquine or NH_4Cl treatment, accumulation of CTFα was observed in *PS1*$^{-/-}$ *PS2*$^{-/-}$ cells (Fig. 1*A*). We were unable to detect CTFβ, which is derived from endogenous APP, likely due to the low β-secretase activity in these cells (Fig. 1*A*). In chloroquine- or NH_4Cl-treated APP_{NL}-H4 cells, we also observed accumulation of both CTFα and AICD with no change in FL-APP (Fig. 1*B*). Conversely, treatment with the γ-secretase inhibitor L-685,458 produced a significant accumulation of CTFs and lower production of AICD in APP_{NL}-H4 cells (Fig. 1*B*).

To address whether the cathepsin family is involved in degrading CTFs and AICD, we treated APP_{NL}-H4 cells with representative cathepsin inhibitors (Fig. 1*C*, *D*). Cathepsins B, D, and G are cysteine, aspartyl, and serine proteases, respectively. E-64d generally inhibits cysteine proteases. Western blot analysis showed that CTFα, CTFβ, and AICD did not significantly accumulate in the presence of inhibitors for cathepsins G and D (cathepsin G inhibitor I and pepstatin A, respectively), but E-64d and the cathepsin B-specific inhibitor CA-074Me markedly increased accumulation of CTFα, CTFβ, and AICD (Fig. 1*C*). In addition, treatment with the proteasome inhibitor lactacystin exerted no significant influence on the levels of CTFα, CTFβ, and AICD production (Fig. 1*C*). It has been reported that cathepsin B prefers wild-type APP (APP_{WT}) to APP_{NL} (12). Although CA-074Me treatment led to significant accumulation of CTFα, CTFβ, and AICD in stably APP_{WT}-overexpressing H4 cells (APP_{WT}-H4 cells), this efficacy in APP_{WT}-H4 cells was less than that observed in APP_{NL}-H4 cells (Supplemental Fig. S1).

If CA-074Me causes up-regulation of both α- and β-secretase activities, CTFα and CTFβ might simultaneously accumulate in cells. To evaluate the effects of CA-074Me on α- and β-secretase activities, sAPPα and sAPPβ levels were assessed in the conditioned medium from APP_{NL}-H4 cells treated with CA-074Me (Fig. 1*E*, *F*). No change in either sAPPα or sAPPβ levels was observed (Fig. 1*F*). Therefore, we concluded that cysteine protease cathepsin B was a major CTF- and AICD-degrading enzyme with no effect on α- and β-secretase activities.

Time course and dose dependency of the accumulation of CTFs and AICD *via* cathepsin B inhibition

To accurately assess the drug efficacy of CA-074Me, we performed time-course and dose-dependency analyses in APP_{NL}-H4 cells (**Fig. 2**). Time-course analysis revealed that CA-074Me treatment for 6 h or longer resulted in the gradual accumulation of CTFα, CTFβ, and AICD, as compared to 0 h of treatment (Fig. 2*A*, *B*). The effect of CA-074Me was observed to differ among CTFα, CTFβ, CTFs, and AICD. The accumulation of CTFα, CTFβ, and CTFs reached a peak at 12 h; in contrast, an accumulation of AICD showed a monotonic increase over a 0- to 24-h period (Fig. 2*A*, *B*). Dose-dependency analysis demonstrated that inhibition of cathepsin B by CA-074Me at 1 μM or more led to a significant accumulation of CTFα, CTFβ, CTFs, and AICD (Fig. 2*C*, *D*).

CA-074 and CA-074Me have no inhibitory effect on γ-secretase activity of the presenilin complex

Several drugs have been reported to inhibit or modulate γ-secretase activity, and nonsteroidal anti-inflammatory

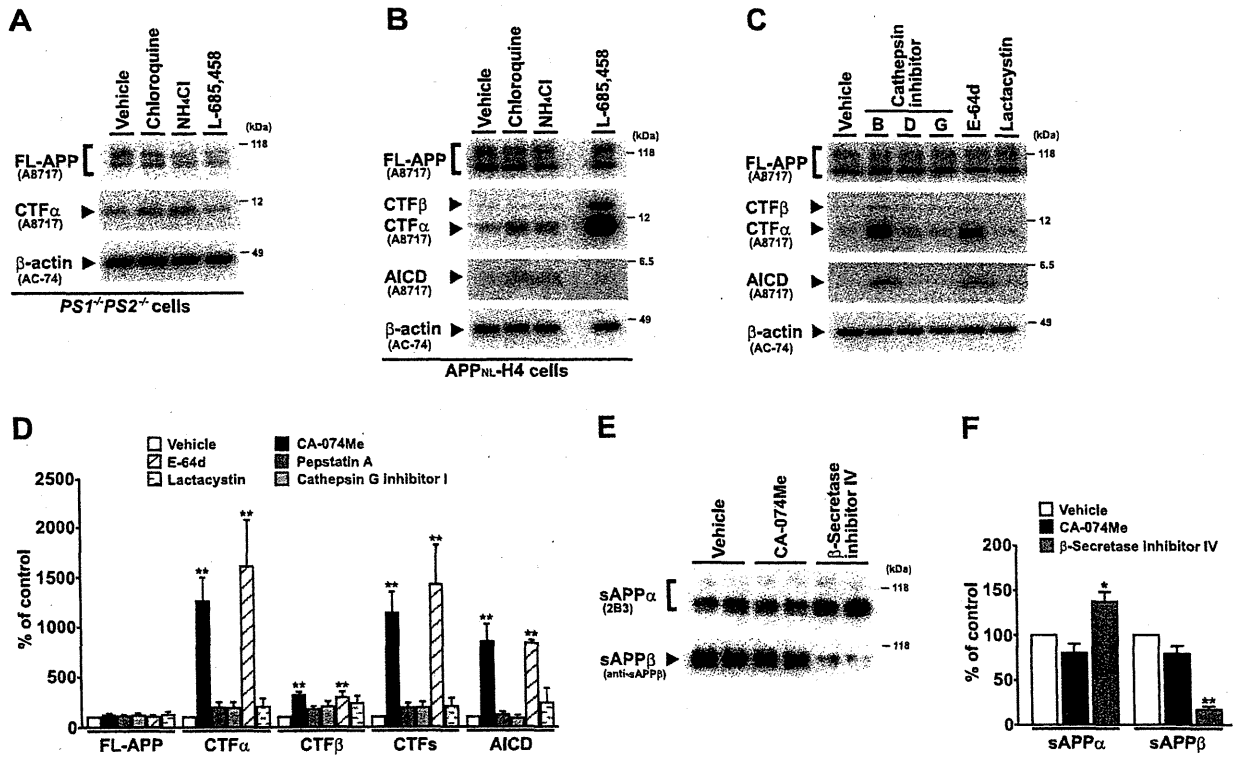

Figure 1. CA-074Me and E-64d lead to the accumulation of CTFs and AICD with no change in α- and β-secretase activities. *A*) Representative Western blots show the effect of treatment with chloroquine (1 μM), ammonium chloride (1 mM), or L-685,458 (1 μM) for 24 h on FL-APP, and CTFα levels in $PS1^{-/-}PS2^{-/-}$ cells. FL-APP and CTFα were detected with A8717; β-actin was detected with AC-74. *B*) Representative Western blots show the effect of treatment with chloroquine (1 μM), ammonium chloride (1 mM), or L-685,458 (1 μM) for 24 h on FL-APP, CTFα, CTFβ, and AICD levels in APP_{NL}-H4 cells. FL-APP, CTFα, CTFβ, and AICD were detected with A8717; β-actin was detected with AC-74. *C*) Amounts of FL-APP, CTFα, CTFβ, and AICD in the cell lysates of APP_{NL}-H4 cells treated with cathepsin inhibitors [B, CA-074Me (10 μM); D, pepstatin A (10 μM); G, cathepsin G inhibitor I (10 μM)], E-64d (10 μM), or lactacystin (1 μM) for 24 h were measured by semiquantitative Western blot analysis. β-Actin was used as loading control (*A–C*). *D*) Results of Western blot analysis shown in *C*. Data represent means ± SE of 5 experiments. $^{**}P < 0.01$: significantly different from the vehicle-treated group. *E*) Amounts of sAPPα or sAPPβ in conditioned medium from APP_{NL}-H4 cells treated with CA-074Me (10 μM) or β-secretase inhibitor IV (1 μM; as a positive control) for 24 h were measured by semiquantitative Western blot analysis with 2B3 or anti-sAPPβ antibody, respectively. *F*) Results of Western blot analysis shown in *E*. Data represent means ± SE of 4 experiments. $^{*}P < 0.05$, $^{**}P < 0.01$ *vs.* vehicle-treated group.

drugs (NSAIDs) are representative γ-secretase modulators that lower Aβ42 production and increase Aβ38 production. To elucidate the effects of CA-074Me on γ-secretase activity, we examined whether CA-074Me has a direct effect on γ-secretase activity (**Fig. 3**). We prepared a total cell membrane fraction of APP_{NL}-H4 cells and incubated this fraction with L-685,458, CA-074Me, or CA-074, which is a nonmethyl esterified analog of CA-074Me. Western blot analysis with anti-APP antibody showed that a γ-secretase inhibitor significantly suppressed production of AICD (Fig. 3*A*, lane 8; *B*). Treatment with cathepsin B-specific inhibitors CA-074 or CA-074Me did not suppress γ-secretase activity in the membrane fraction, as compared to treatment with vehicle (Fig. 3*A*, lane 3 *vs.* 4–7; *B*). Similarly, Western blot analysis with the antibody 82E1 showed that both CA-074 and CA-074Me failed to block production of Aβ (Fig. 3*C*, lane 3 *vs.* lanes 4–7, *D*). However, L-685,458 inhibited γ-secretase activity, leading to a decrease in Aβ levels, as compared to vehicle (Fig. 3*C*, lane 8; *D*). A weak band (Fig. 3*C*, lane 8) is believed to be Aβ preexisting in the membrane fraction (Fig. 3*C*, lane 2, bottom band of Aβ), and new Aβ was processed from longer Aβ (Fig. 3*C*, lane 2, top band of Aβ). This observation is consistent with a previous report that suggests longer Aβ can be processed to shorter Aβ by γ-secretase in the presence of L-685,458 without production of AICD (21). These results clearly demonstrate that the cathepsin B-specific inhibitors CA-074 and CA-074Me did not significantly affect the activity of γ-secretase.

Inhibition of cathepsin B has no inhibitory effect on Notch processing

With a rare exception, all γ-secretase substrates are membrane-associated stubs, which are type I membrane proteins with ectodomain shedding. The intracellular domain of several γ-secretase substrates cleaved by γ-secretase translocates into the nucleus, and this domain has been shown to activate transcription. To assess the effect of CA-074Me on the processing of Notch, another γ-secretase substrate, we treated $mNotch^{\Delta E}$-

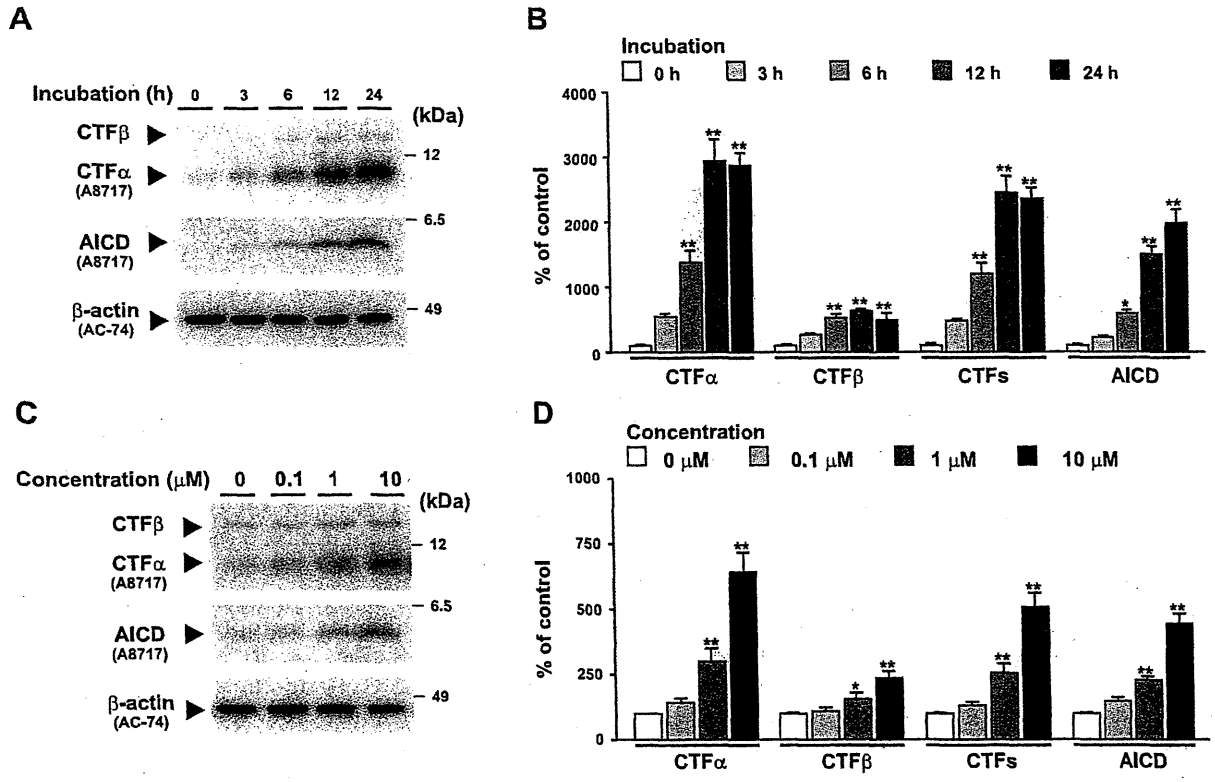

Figure 2. Inhibition of cathepsin B leads to the time- and dose-dependent accumulation of CTFs and AICD. *A*) Amounts of CTFα, CTFβ, and AICD in the cell lysates of APP_{NL}-H4 cells treated with CA-074Me (10 μM) for 0, 3, 6, 12, or 24 h were measured by semiquantitative Western blot analysis with A8717. *B*) Results of Western blot analysis shown in *A*. *C*) Amounts of CTFα, CTFβ, and AICD in the cell lysates of APP_{NL}-H4 cells treated with CA-074Me (0, 0.1, 1, or 10 μM) for 24 h were measured by semiquantitative Western blot analysis with A8717. *D*) Results of Western blot analysis shown in *C*. β-Actin was used as loading control and detected with AC-74 (*A*, *C*). Data represent means ± SE of 4 experiments. $*P < 0.05$, $**P < 0.01$ *vs.* control treatment group.

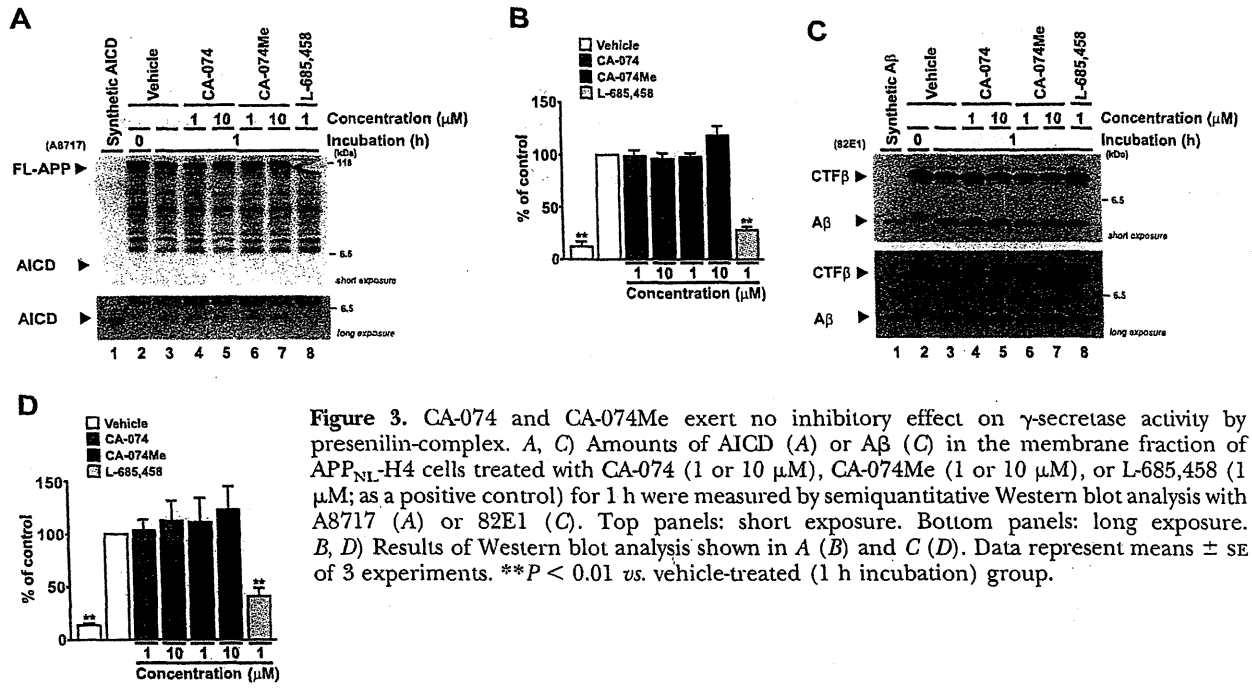

Figure 3. CA-074 and CA-074Me exert no inhibitory effect on γ-secretase activity by presenilin-complex. *A*, *C*) Amounts of AICD (*A*) or Aβ (*C*) in the membrane fraction of APP_{NL}-H4 cells treated with CA-074 (1 or 10 μM), CA-074Me (1 or 10 μM), or L-685,458 (1 μM; as a positive control) for 1 h were measured by semiquantitative Western blot analysis with A8717 (*A*) or 82E1 (*C*). Top panels: short exposure. Bottom panels: long exposure. *B*, *D*) Results of Western blot analysis shown in *A* (*B*) and *C* (*D*). Data represent means ± SE of 3 experiments. $**P < 0.01$ *vs.* vehicle-treated (1 h incubation) group.

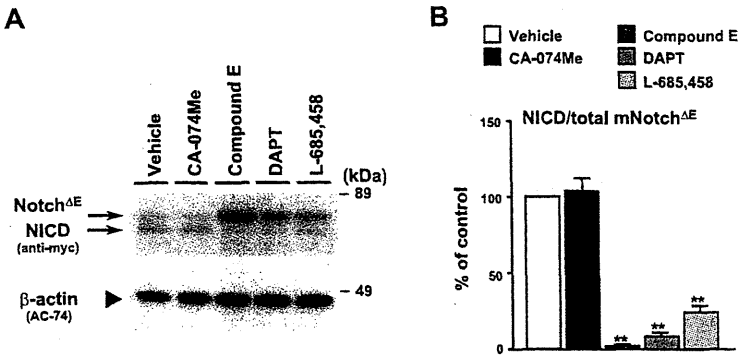

Figure 4. Inhibition of cathepsin B has no inhibitory effect on Notch processing. *A*) Amounts of Notch fragments in the cell lysates of mNotch$^{\Delta E}$-N2a cells treated with CA-074Me (10 μM) or γ-secretase inhibitors (compound E, DAPT, and L-685,458; 1 μM) for 24 h were measured by semiquantitative Western blot analysis with anti-myc antibody. Sample Western blots for mNotch$^{\Delta E}$ and NICD are shown. β-Actin was used as loading control and detected with AC-74. *B*) Results of Western blot analysis shown in *A*. Data represent means ± SE of 4 experiments. $^{**}P < 0.01$ *vs.* vehicle-treated group.

N2a cells, which were stably overexpressing ectodomain truncated mouse Notch$^{\Delta E}$, with CA-074Me or typical γ-secretase inhibitors (compound E, DAPT, and L-685,458; **Fig. 4**). Western blot analysis indicated that treatment with compound E, DAPT, or L-685,458 significantly inhibited Notch processing, leading to a decrease in production of the Notch intracellular domain (NICD), as compared to treatment with vehicle. However, treatment with CA-074Me had no significant effect on the production of NICD. From these data, we conclude that cathepsin B, unlike APP, barely influences regulated intramembrane proteolysis of Notch or degradation of NICD.

Cathepsin B is involved in the metabolism of CTFs independently of γ-secretase

Our results clearly suggest that cathepsin B and γ-secretase separately catalyze the proteolysis of CTFα and CTFβ, based on the following observations: chloroquine and NH_4Cl caused accumulation of CTFα in *PS1*$^{-/-}$*PS2*$^{-/-}$ cells; inhibition of cathepsin B caused accumulation of CTFs and AICD in APP$_{NL}$-H4 cells; and CA-074Me did not inhibit γ-secretase activity in the membrane fraction. To ascertain this conclusion, we investigated the effect of a combination of CA-074Me and γ-secretase inhibitor (compound E or L-685,458) in APP$_{NL}$-H4 cells (**Fig. 5*A*, *B***). Western blot analysis demonstrated that CTFs significantly accumulated following treatment with CA-074Me alone, γ-secretase inhibitor alone, or both of these compounds. Compound E is a peptidomimetic nontransition-state γ-secretase inhibitor, and L-685,458 is a hydroethylene dipeptide isostere-type transition-state analog. CA-074Me caused additional accumulation of CTFs in the presence of γ-secretase inhibitor; however, there was no difference in the level of extracellular Aβ, which is

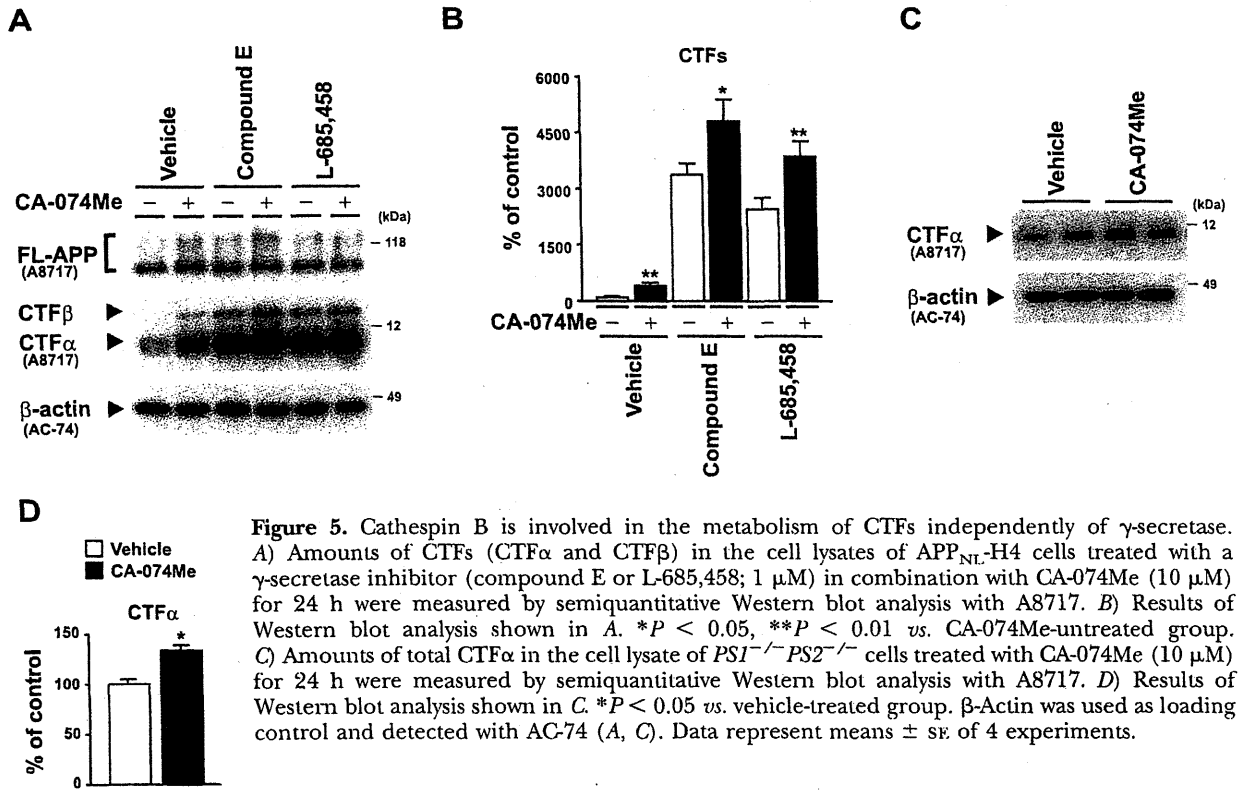

Figure 5. Cathepsin B is involved in the metabolism of CTFs independently of γ-secretase. *A*) Amounts of CTFs (CTFα and CTFβ) in the cell lysates of APP$_{NL}$-H4 cells treated with a γ-secretase inhibitor (compound E or L-685,458; 1 μM) in combination with CA-074Me (10 μM) for 24 h were measured by semiquantitative Western blot analysis with A8717. *B*) Results of Western blot analysis shown in *A*. $^{*}P < 0.05$, $^{**}P < 0.01$ *vs.* CA-074Me-untreated group. *C*) Amounts of total CTFα in the cell lysate of *PS1*$^{-/-}$*PS2*$^{-/-}$ cells treated with CA-074Me (10 μM) for 24 h were measured by semiquantitative Western blot analysis with A8717. *D*) Results of Western blot analysis shown in *C*. $^{*}P < 0.05$ *vs.* vehicle-treated group. β-Actin was used as loading control and detected with AC-74 (*A*, *C*). Data represent means ± SE of 4 experiments.